ELSEVIER

Marine Geology 192 (2002) 23–58

MARINE GEOLOGY
INTERNATIONAL JOURNAL OF MARINE GEOLOGY, GEOCHEMISTRY AND GEOPHYSICS

www.elsevier.com/locate/margeo

Variability in form and growth of sediment waves on turbidite channel levees

William R. Normark [a,*], David J.W. Piper [b], Henry Posamentier [c], Carlos Pirmez [d], Sébastien Migeon [b]

[a] *Coastal and Marine Geology, U.S. Geological Survey, Menlo Park, CA 94025, USA*
[b] *Geological Survey of Canada (Atlantic), Dartmouth, NS, Canada B2Y 4A2*
[c] *Anadarko Canada Corporation, Calgary, AB, Canada T2P 4V4*
[d] *Shell International Exploration and Production Inc., Houston, TX 77001, USA*

Received 30 January 2001; received in revised form 23 October 2001; accepted 2 August 2002

Abstract

Fine-grained sediment waves have been observed in many modern turbidite systems, generally restricted to the overbank depositional element. Sediment waves developed on six submarine fan systems are compared using high-resolution seismic-reflection profiles, sediment core samples (including ODP drilling), multibeam bathymetry, 3D seismic-reflection imaging (including examples of burried features), and direct measurements of turbidity currents that overflow their channels. These submarine fan examples extend over more than three orders of magnitude in physical scale. The presence or absence of sediment waves is not simply a matter of either the size of the turbidite channel-levee systems or the dominant initiation process for the turbidity currents that overflow the channels to form the wave fields. Both sediment-core data and seismic-reflection profiles document the upslope migration of the wave forms, with thicker and coarser beds deposited on the up-current flank of the waves. Some wave fields are orthogonal to channel trend and were initiated by large flows whose direction was controlled by upflow morphology, whereas fields subparallel to channel levees resulted from local spillover. In highly meandering systems, sediment waves may mimic meander planform. Larger sediment waves form on channel-levee systems with thicker overflow of turbidity currents, but available data indicate that sediment waves can be maintaned during conditions of relatively thin overflow. Coarser-grained units in sediment waves are typically laminated and thin-bedded sand as much as several centimetres thick, but sand beds as thick as several tens of centimetres have been documented from both modern and buried systems. Current production of hydrocarbons from sediment-wave deposits suggests that it is important to develop criteria for recognising this overbank element in outcrop exposures and borehole data, where the wavelength of typical waves (several kilometres) generally exceeds outcrop scales and wave heights, which are reduced as a result of consolidation during burial, may be too subtle to recognise.

Keywords: sediment wave; turbidite; lithology; planform; depositional processes

* Corresponding author. Tel.: +1-650-329-5200; Fax: +1-650-329-5198.
E-mail addresses: wnormark@usgs.gov (W.R. Normark), piper@agc.bio.ns.ca (D.J.W. Piper), henry_posamentier@anadarko.com (H. Posamentier), carlos.pirmez@shell.com (C. Pirmez), migeon@agc.bio.ns.ca (S. Migeon).

0025-3227/02/$ – see front matter
PII: S0025-3227(02)00548-0

1. Introduction

Large-scale fine-grained sediment waves are widespread in turbidite systems, being particularly well developed on the right-hand levee of submarine fan valleys (and on left-hand levees in the southern hemisphere: Normark et al., 1980; Carter and Carter, 1987; Carter et al., 1990). The waves typically are 3–20 m high and have wavelengths of 300–6000 m. Limited data suggest that sediment waves are commonly linear to slightly sinuous and oblique to channel orientation (Migeon et al., 2000; McHugh and Ryan, 2000; Wynn et al., 2000a), so that they may result either from local levee spillover or from more regional overbanking turbidity current flow. The wave forms vary from typical asymmetric sediment waves that show up-flow migration, to more symmetric waves that grow by aggradation (defined here as horizontal migration <5 times vertical accretion), as described by Migeon et al. (2000) from the Var Fan. A single wave may at different times be dominated by horizontal migration or by vertical aggradation (Skene, 1998). The waves are built of typical overbank turbidite sediment, principally millimetre to centimetre beds of fine sand and silt and decimetre beds of turbidite mud. Sediment waves of similar morphology are also found on sediment drifts formed by contour currents (Flood, 1988; Faugères and Stow, 1993; Howe, 1996).

Two approaches have been used to analyse flow conditions that lead to sediment wave formation. One is that the sediment waves develop beneath standing waves that form at the upper interface of a turbidity current (Normark et al., 1980). The other is that standing waves may develop even where no sharp density or velocity gradient exists, as in the development of sediment waves on sediment drifts formed by oceanic thermohaline circulation (Flood, 1988). In both cases, there are internal structures in the flow that are similar in wavelength to the sediment waves and flow over such bedforms is analogous to flow over antidunes reported from laboratory channels. Flow in both analyses can be characterised by a densiometric Froude number, with values of about 1.

The purpose of this paper is two-fold. First, from the comparison of several case studies, to better understand the variability in distribution and architecture of fine-grained sediment waves in turbidite systems and hence to better understand their origin. Second, to identify where thick sand beds that might be important as hydrocarbon reservoirs are found in sediment waves, using a review of cores and high-resolution seismic-reflection profiles available for several of the case studies.

These objectives are achieved by reviewing a series of examples. First the planform morphology of turbidite-levee sediment waves is described from multibeam bathymetric imagery of Monterey Fan, in order to relate sediment wave distribution to channel pattern and to the sediment character revealed by piston and free-fall cores from the sediment-wave fields. The Monterey data are compared with results from other studies of sediment wave planform from the literature. This information on planform character is used to constrain the interpretation of levee sediment waves in seismic-reflection profiles. Two contrasting turbidite systems have been studied, Amazon and Hueneme fans, for which there is independent evidence for changes in the size and sediment load of turbidity currents over the past few tens of thousands of years (Piper and Normark, 2001). Variations in sediment-wave scale and architecture in time and space are related to inferred flow conditions of turbidity currents on the fans. Variability in sand and silt beds from closely spaced ODP holes on Amazon Fan is examined. The hypotheses proposed on the basis of these data are then tested using morphometric data from other levee sediment-wave systems offshore Nigeria and Indonesia that have been imaged in 3D seismic-reflection data. Sediment waves are described from Reserve Fan in Lake Superior, where measurements of the behaviour of turbidity currents are available (Normark, 1989; Normark and Dickson, 1976a). Finally, the role of overbank levee sand as a potential hydrocarbon reservoir is evaluated, particularly the thicker sand beds deposited in the early phase of sediment-wave development.

2. Results

2.1. Monterey Fan

The Upper Turbidite System of Monterey Fan (UTS; Normark, 1999) accumulated in the last 0.5 Ma from sediment transported through Monterey and Ascension canyons (Fig. 1). The UTS overlies older turbidite systems with different sources, including Pioneer canyon to the north (Fig. 1; Fildani, 1993). Widespread sediment waves have been recognised in overbank areas along both active and abondoned fan valleys on Monterey Fan. Multibeam bathymetric data collected by NOAA (Greene and Hicks, 1990) show that fields of sediment waves are developed: (1) on the western levee of Ascension Fan valley and the contiguous area of the western levee of Monterey Fan valley, (2) downstream from the Shepard meander (Shepard, 1966) on the southern levee of Monterey Fan valley, (3) on both levees of Pioneer Fan valley (although best developed on the western levee), and (4) on the northwest levee of an abandoned leveed-valley immediately west of Monterey Fan valley (Fig. 1). Sediment waves downslope from the Shepard meander of Monterey Fan valley have recently been studied by McHugh and Ryan (2000).

The sediment-wave fields on the western levees of Pioneer and Ascension Fan valleys both occur where the upper fan valley takes a sharp left bend. The waves are essentially concentric about these bends (Fig. 1), suggesting that they formed by spreading spillover flows from the bends. Wavelengths are generally 2–3 km and wave heights appear to decrease down-fan. Sediment waves south of the Shepard meander, which are likewise approximately concentric and subparallel to a pronounced loop in the channel, decrease in size away from the channel much faster than those along straight channel segments, presumably because of the effects of spreading flow (McHugh and Ryan, 2000).

Sediment waves on the western levee of Monterey Fan valley to the west of and downstream from the Shepard meander are oriented slightly oblique to the channel (with the sinuous wave crests generally trending within 20° of the trend of the levee crest). Seismic-reflection profiles (Fig. 2) show that sediment waves characterise the western levee throughout the UTS, although at the base of the system, some troughs appear to have migrated away from the channel.

One small area of the Monterey valley western levee was investigated in detail by Normark et al. (1980), and some of their data are re-examined here. A detailed bathymetric survey shows that at least the smaller sediment waves are laterally discontinuous features (Fig. 3), a characteristic also seen in larger waves in multibeam imagery (see west levee of Pioneer Fan valley in Fig. 1). The 3.5-kHz profile in Fig. 4 shows >50 m penetration and progressive migration of crests and troughs towards the fan valley, with the rate of migration of crests greater than that of troughs. Internal reflectors can be correlated in most cases from one flank to another, showing that sediment thickness is 2–3 times higher on the up-current flank but that no systematic thickness variations are visible between proximal and distal sediment waves. Some strata are truncated on the down-current flanks, mostly those close to the present sea floor. At some stratigraphic horizons, reflection amplitude is substantially greater on the up-current flank, including reflections close to the present seabed (Fig. 4).

Free-fall gravity cores (Fig. 5A) sampled mud with a correlatable horizon of silt beds and laminae (Normark et al., 1980). A correlatable late Holocene colour change at about 0.5 mbsf is related to sediment source, not diagenesis. Sediment thickness above the colour change is greatest on the up-current side of waves and least on the down-current slopes and crest. A 1–2-cm-thick sandy silt bed is found only on the up-current side and at the extreme crest of the waves; in all other cores, only thin silty laminae are present.

A longer stratigraphic record is revealed by piston cores (Fig. 5B). All of these cores were attempted from near the crest of waves, at increasing distance across the levee from the fan valley (Fig. 2). Correlations using the late Holocene colour change and the biostratigraphically determined marker close to the Holocene–Pleistocene boundary show that thickness variations resulting from the position on the waves probably mask

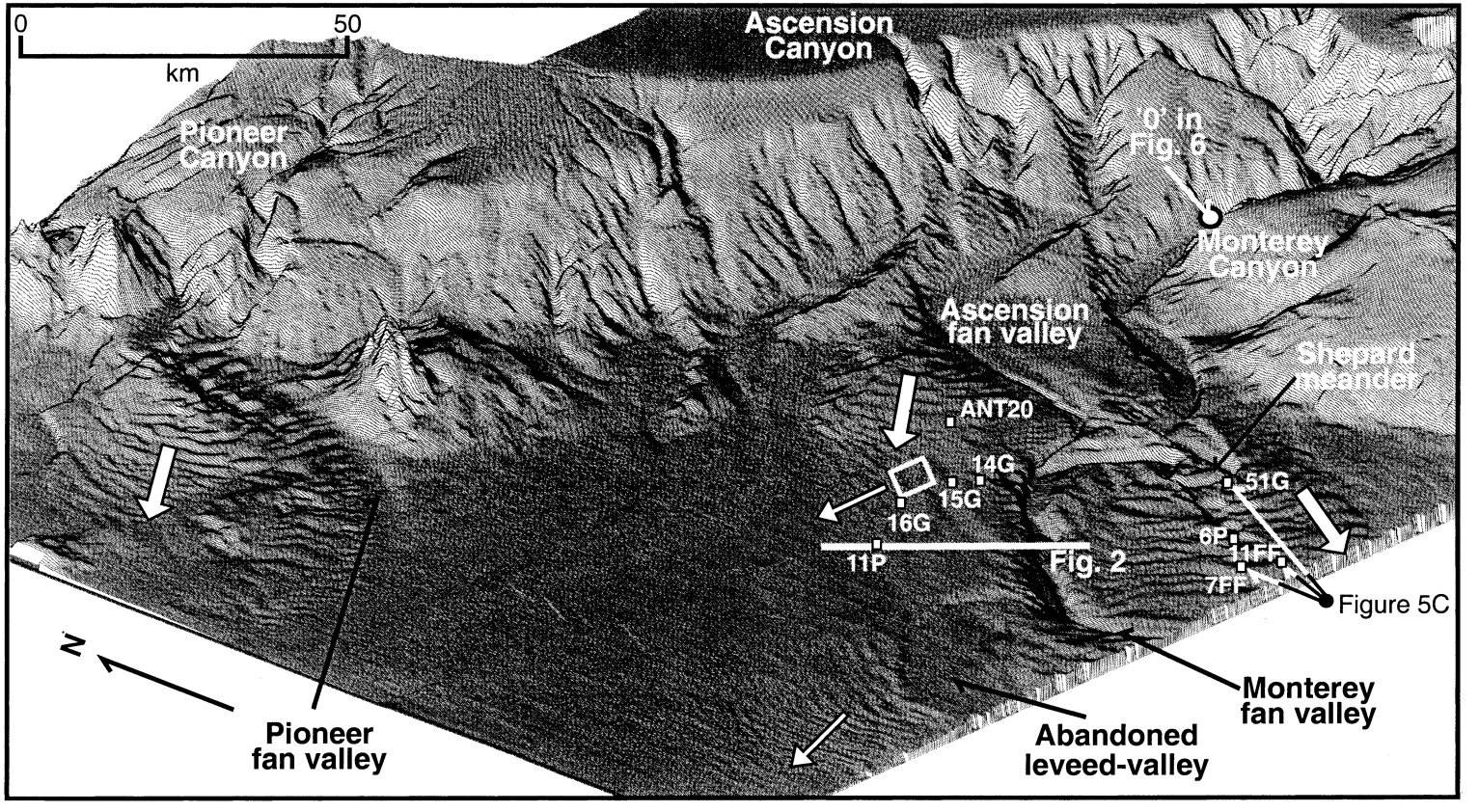

Fig. 1. Multibeam shaded-relef oblique view of Monterey Fan (modified from Greene and Hicks, 1990) showing large-scale sediment-wave features. Large white arrows show wave fields (from left to right) of Pioneer Fan valley, Ascension Fan valley, and overflow from the Shepard meander in Monterey Fan valley. Narrow white arrows show areas of smaller waves associated with Monterey Fan valley and an abandoned leveed valley. Area of Fig. 3 (small box), seismic-reflection profile of Fig. 2, and location of cores in Fig. 5B,C are shown. A white-filled circle marks the upstream end of the longitudinal profiles of channel and levee depths in Fig. 6A.

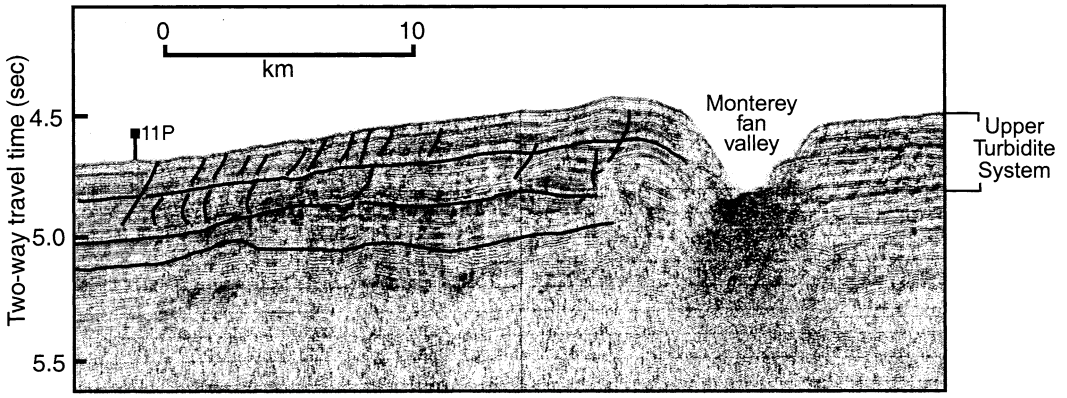

Fig. 2. Seismic-reflection profile across the modern Monterey leveed channel of the Upper Turbidite System (Normark, 1999) showing evolution of sediment waves. Position of core 11P is shown. Location of profile shown in Fig. 1.

any variations with distance from channel. In cores with a thicker Holocene section, the number of Holocene sandy silt and sand beds is also greater (compare core 16G with core 15G).

Cores down-fan from the main loop of the Shepard meander (Fig. 5C and core 6P in Fig. 5B) have more abundant and thicker sand beds in the mid to late Holocene interval than cores of similar age on the western levee, presumably because of the lower levee height in this reach of the channel (Fig. 6A). Sand beds up to 17 cm thick were sampled with both piston and gravity cores. The lateral continuity of these sands is not known.

Two basic types of sediment waves are found on Monterey Fan: large sediment waves formed at (and concentric around) major flow stripping sites associated with sharp bends in the channels; and smaller up-flow migrating sediment waves that are oblique to the channel trend and formed on the backsides of the higher right-hand levee of gently curving channels. Available core data from the smaller sediment waves show that sand beds are more uniform in thickness on the levee crest whereas lenticular sand beds and starved ripples are common in the area of the large sediment waves. The numerous sand and silt beds deposited during the Holocene show that many turbidity currents thicker than 400 m (the relief of the adjacent channel) were initiated during sea level rise. Normark et al. (1980) suggested that the thickness of the overbank flows in the area of the sediment wave field might have been as much as 800 m.

2.2. Hueneme Fan

Hueneme Fan (Fig. 7) is a small sandy submarine fan offshore Los Angeles fed principally by the Santa Clara River delta and longshore drift of sediment. High-resolution airgun seismic-reflection profiles (Normark et al., 1998) and Huntec boomer profiles with 0.4 m vertical resolution (Piper et al., 1999) are available on a grid with 2–5 km spacing. Chronology is by correlation with ODP Site 1015 (Fig. 8A). Sparse piston cores provide ground truth for acoustic facies recognised in boomer profiles. Stratigraphic nomenclature is summarised by Normark et al. (1998) and Piper et al. (1999), who defined a series of reflectors from A to O in decreasing order of age (Fig. 8A,B). In addition a reflector N′, between N and O, is recognised in this study. On Hueneme Fan, changes have occurred since the late Pleistocene in both the initiation processes for turbidity currents (Fig. 8A) and the overall size of turbidity currents (Fig. 8C). The evolution of sediment waves is studied in the context of these changes.

The main fan valley leads from Hueneme canyon and has been active continuously for at least the past 13 ka. The levees are highly asymmetric, with the western (right-hand looking down-flow) levee consisting of a high main levee and an inner levee that developed in the early Holocene (Fig. 8C) as flow volume decreased (Piper and Normark, 2001). Sediment waves are ubiquitous on the right-hand levee of Hueneme Fan valley

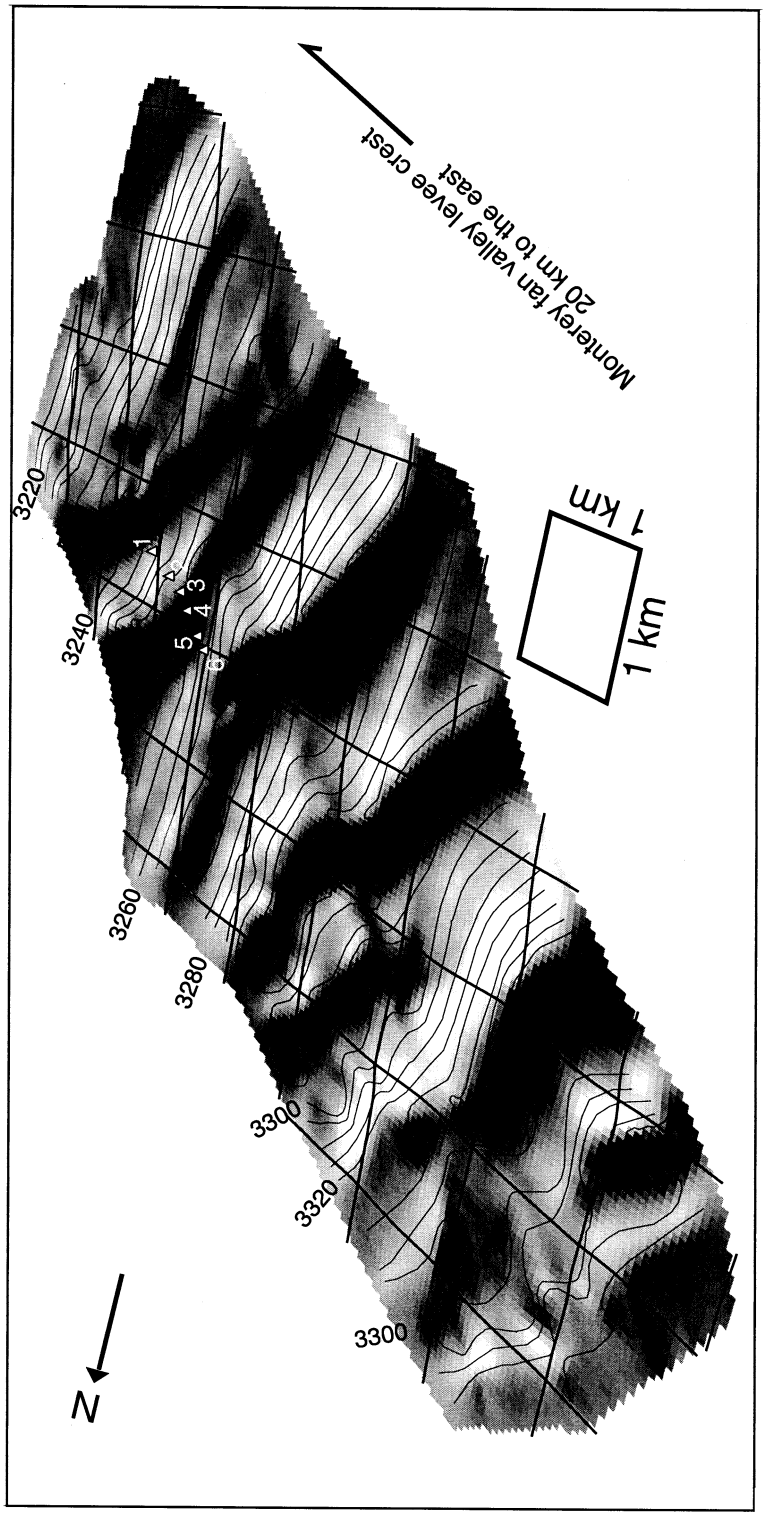

Fig. 3. Shaded relief oblique view with bathymetric contours of the sediment-wave field of western levee of Monterey Fan valley showing location of free-fall cores depicted in Fig. 5A. Modified from Normark et al. (1980). Location in Fig. 1.

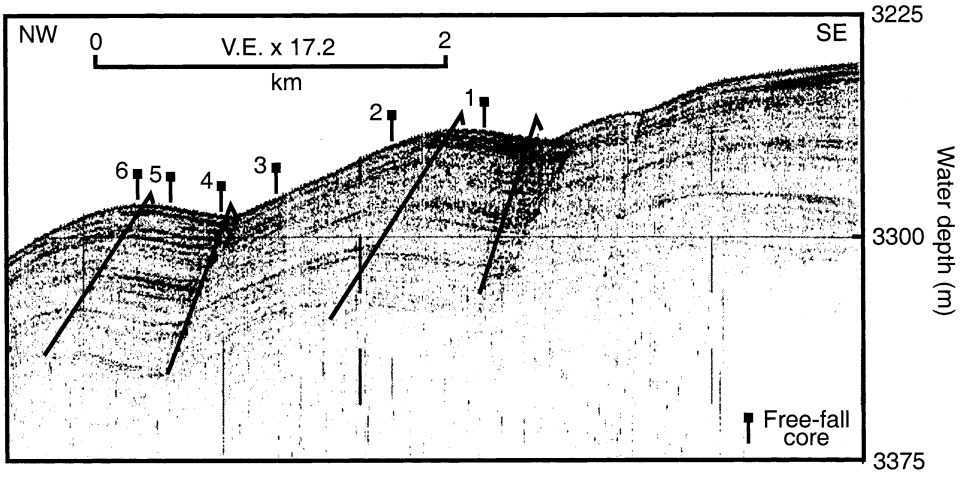

Fig. 4. 3.5-kHz profile of sediment waves on western levee of Monterey Fan valley showing the position of gravity cores, which lie along the profile, in Fig. 5A. Arrows show migration of sediment-wave crests and troughs.

(Figs. 9 and 10). Observations on both dip and strike seismic-reflection lines suggest that the waves are somewhat oblique to the fan valley, as in the case of Monterey Fan. They also confirm that variations in the ratio of horizontal migration to aggradation are not a result of changes in orientation of the waves.

Sediment waves on Hueneme Fan show a repetitive pattern, developed at three stratigraphic levels. Early in their history, waves have high rates of up-current migration relative to aggradation, but this ratio diminishes when passing stratigraphically upward. At the same time, slopes generally decrease. The oldest level showing such a pattern is beneath the main levee, from 650 to 790 mbsl, immediately above reflector J (Fig. 9), at the top of an extensive sand body deposited at the last glacial maximum. Here the rate of migration is greatest in well-stratified acoustic facies, but diminishes in more transparent facies. Sediment waves appear to have formed above irregularities on the underlying sand facies, perhaps resulting from erosional scours (cf. Normark and Piper, 1991).

The second level is seen on the distal main levee, which prograded across this sand deposit, between reflector M to near reflector N (Figs. 10A and 8B) dating from approximately 8–5 ka (Piper and Normark, 2001). At the same time, on the parts of the levee farther away from the channel, growth of waves was more aggradational (e.g. on the levee in Fig. 9). Stratigraphically overlying wave forms generally are aggradational, with almost no change in trough and crest position (Fig. 10A,B).

The third occurrence is above reflector N′, where waves are developed on the inner levee close to the fan valley, above the apparent planar surface of a sandy channel facies. No irregularities are visible in the underlying sandy facies (Fig. 10D) that might have initiated the wave forms. Wavelength decreases down-valley from 340 m (Fig. 10C) to 150 m (Fig. 10D). The GLORIA long-range sidescan imagery of the fan (EEZScan 84 Scientific Staff, 1986) shows indistinct linear features on the inner levee almost orthogonal to the channel with an average spacing of about 1 km (Fig. 7), probably corresponding to the more prominent waves illustrated in Fig. 10C.

The progressive decrease in up-flow migration of the waves is accompanied by several morphological changes. In the waves at the north end of Fig. 10C, for example, the up-current side becomes gradually steeper (particularly on the northern wave) with some erosion on the lower part of the down-current side. Erosion may be accentuated by spillover between the central and southern wave (Fig. 10C). Similar migration and steepening of the up-current side is shown by the wave in Fig. 10A below reflector N, but above

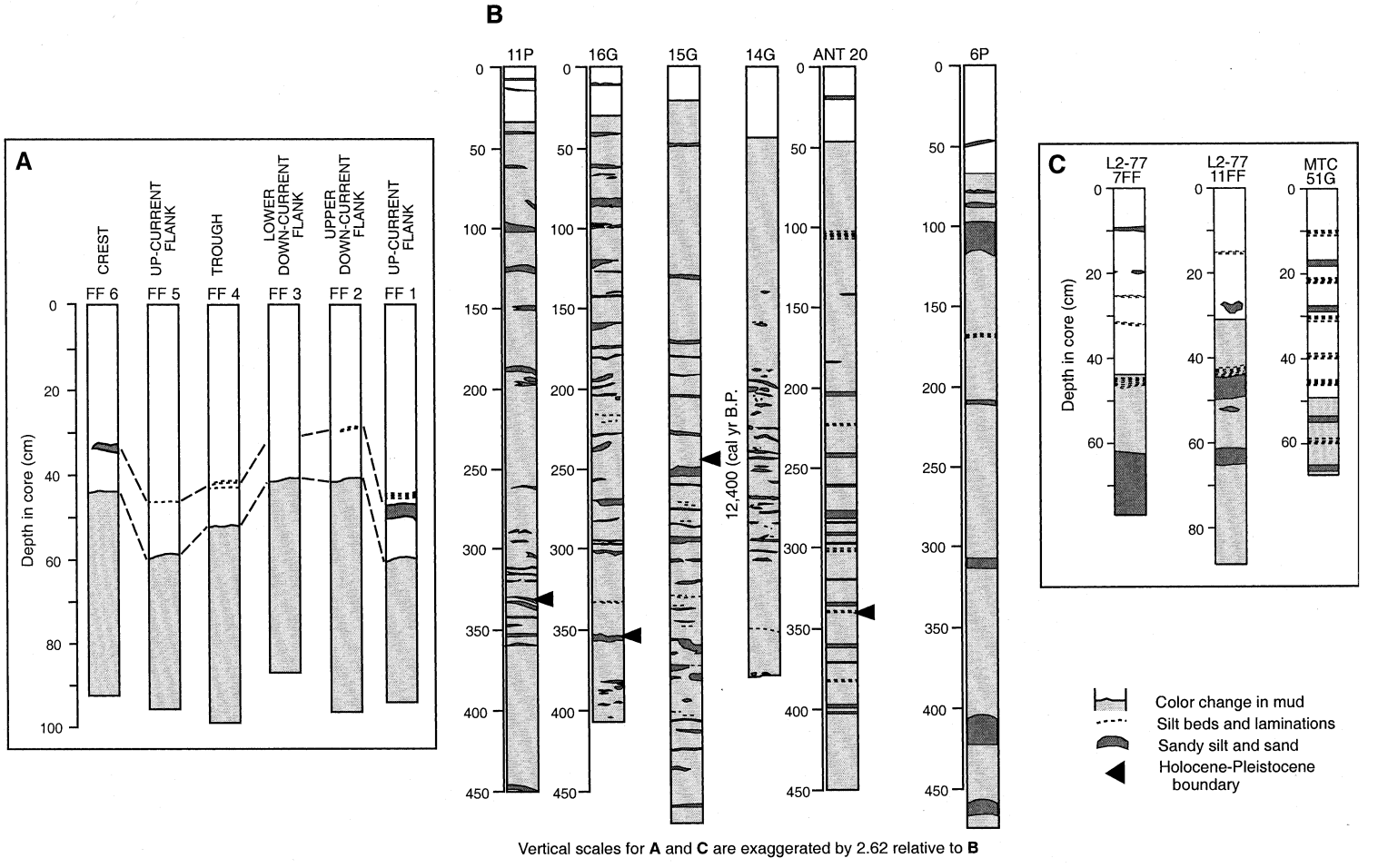

Fig. 5. Detailed sediment logs constructed from descriptions of free-fall, gravity, and piston cores across sediment-wave fields on Monterey Fan. (A) Free-fall (boomerang) cores on western levee (located in Figs. 3 and 4); (B) piston and long gravity cores from western levee (located in Figs. 1 and 2); core S15-79-6P located south of the Shepard meander (Fig. 1); (C) free-fall and gravity cores south of Shepard meander (located in Fig. 1). 'Holocene/Pleistocene' boundary compiled from Hein and Griggs (1972) for core ANT 20, Brunner and Normark (1985) for cores 1P and 16G, and McGann (1990) for core 15G. McGann (pers. commun.) has recently dated the 'Holocene/Pleistocene' boundary at 12 400 cal. yr BP in core 15G.

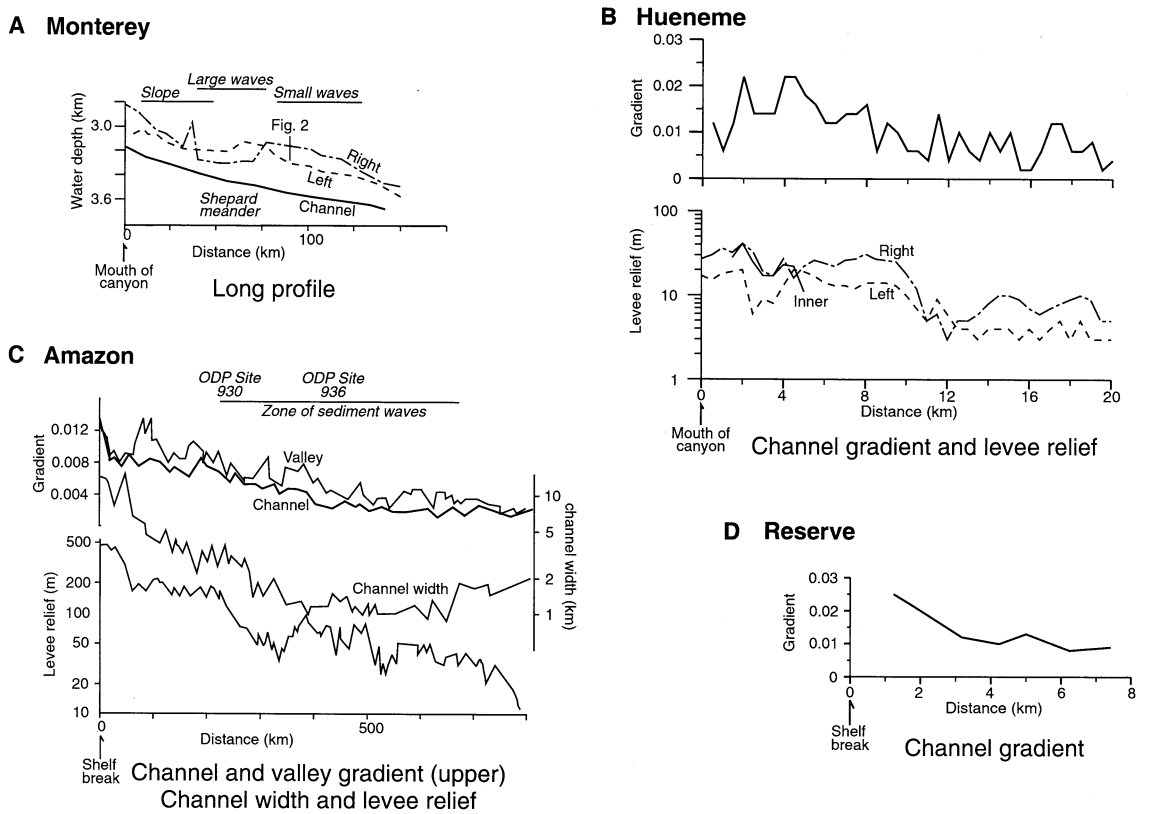

Fig. 6. Along-channel plots of channel width and gradient and levee heights and gradients for (A) Monterey (partly from McHugh and Ryan, 2000), (B) Hueneme, (C) Amazon (Pirmez and Flood, 1995), and (D) Reserve fans showing the distribution of sediment waves.

this a uniform drape was deposited. In the small waves illustrated in Fig. 10D, both crest and trough migrate up-flow, but as the up-current side steepens, the amount of crestal migration is reduced.

On the inner levee, sediment waves interfinger with thicker sand bodies representing periods of channel widening (Figs. 10B and 8B). Boomer profiles show interpreted sand beds up to 3 m thick that pinch out away from the channel. The troughs of some waves show erosion (e.g. the southern troughs in Fig. 10C) and acoustic evidence of sand deposits (figure 7a of Piper et al., 1999). Such evidence for thick sand units is found only within a few kilometres of the fan valley.

Similarly to Monterey Fan, sediment-wave deposition was common during the Holocene on the right-hand levee of an arcuate channel. The Hueneme study shows that sediment waves are interbedded with sandier overbank subelements in addition to the more common occurrence on high muddy levees. The widespread migration and vertical growth of waves above horizon M to close to N took place during incision of the canyon and upper fan valley and the narrowing of the fan valley by deposition of the inner levee (Fig. 8C). Aggradation of waves around horizon N was concurrent with local erosion, and thick sand beds were deposited on the inner levee and on the mid-fan. Migration and vertical growth of waves close to the modern channel also took place above reflector N′ (Fig. 10C) and – most markedly – above horizon O (Fig. 10C,D) at a time when erosion was widespread on the levee adjacent to the upper fan valley (Fig. 10B) as well as on the

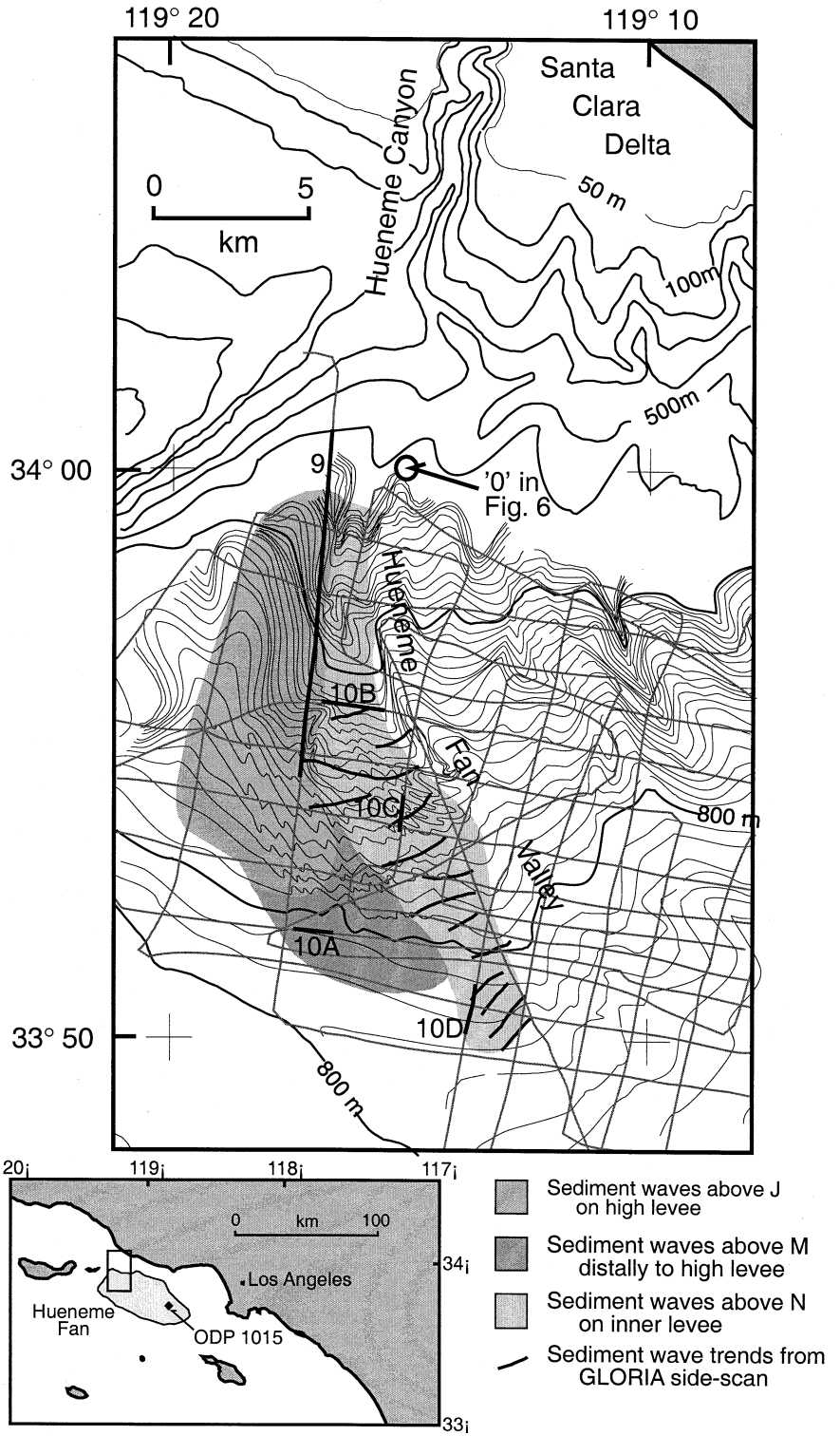
119° 20
119° 10
Santa
Clara
Delta
Hueneme Canyon
0
5
km
50 m
100m
500m
34° 00
9
'0' in
Fig. 6
Hueneme
Fan
10B
10C
800 m
Valley
10A
33° 50
10D
800 m
120i
119i
118i
117i
0 km 100
34i
33i
Los Angeles
Hueneme
Fan
ODP 1015
Sediment waves above J
on high levee
Sediment waves above M
distally to high levee
Sediment waves above N
on inner levee
Sediment wave trends from
GLORIA side-scan

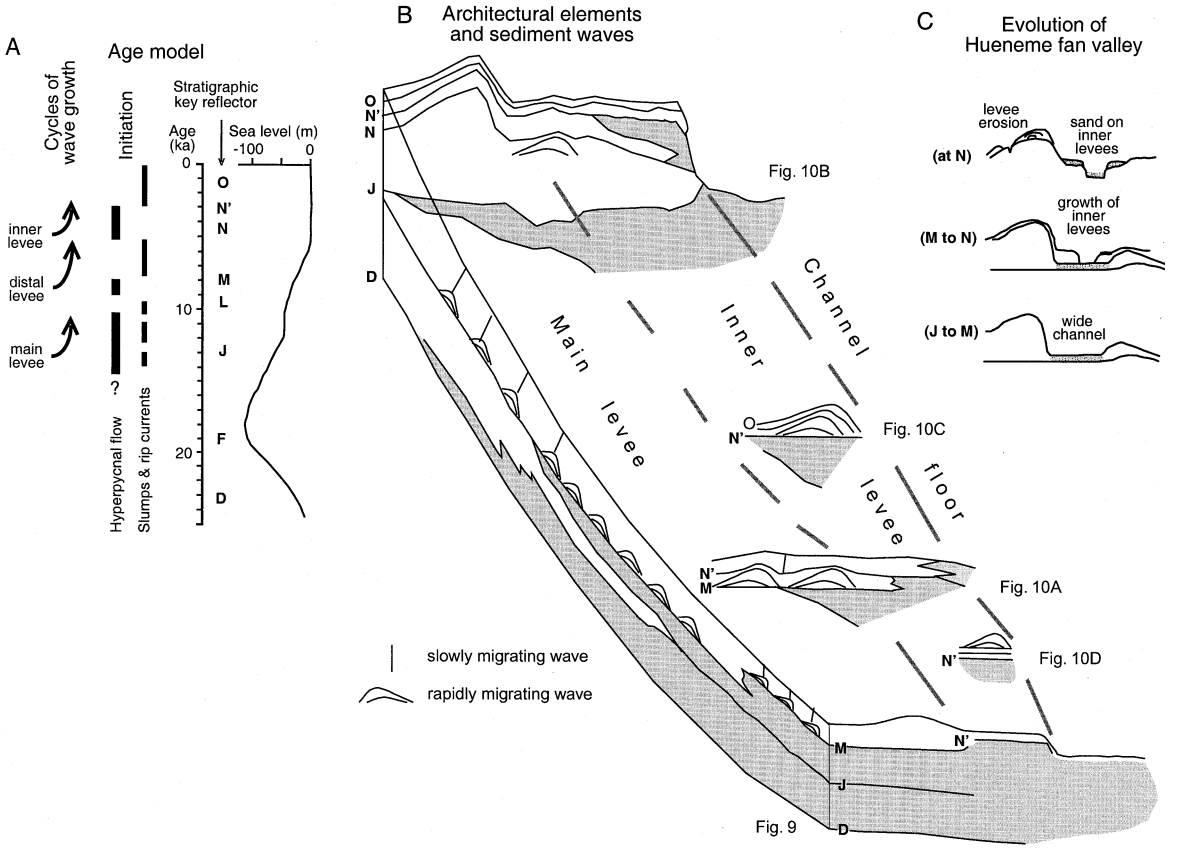

Fig. 8. Stratigraphic cartoon of Hueneme Fan valley showing (A) age of key reflectors, sea-level change, cycles of sediment wave growth and types of initiation of turbidity currents (modified from Piper and Normark, 2001); (B) schematic section of main levee and inner levee showing distribution of sands and sediment waves through the Holocene and late Pleistocene; (C) summary of evolution of Hueneme Fan valley and levees through time.

mid-fan lobes (scoured acoustic facies VIII of Piper et al., 1999). Piper et al. (1999) inferred that hyperpycnal flow was important prior to horizon M and around horizon N, which was when waves were predominantly aggradational. Slump or rip-current-generated turbidity currents predominated between horizons M and N and above O (Fig. 8A), when migration and vertical growth of sediment waves near the fan valley was greatest.

2.3. Amazon Fan

Amazon Fan (Fig. 11) is a large, passive-margin fan fed by the Amazon River at low sea level stands. The upper fan consists of a series of stacked aggradational channel-levee systems. The youngest system is termed Amazon Channel; successively older systems have been given colour names (Brown, Aqua, Purple, Blue, Yellow and

Fig. 7. Map of Hueneme Fan (modified from Piper et al., 1999) showing pattern of sediment-wave distribution and location of illustrated profiles. The stratigraphy of sediment-wave occurrence is based on seismic-reflection profiles. Crests of major sediment waves are interpreted from GLORIA imagery (EEZScan Scientific Party, 1986). Bathymetry and survey track lines from Normark et al. (1998): note that detailed bathymetric interpretation of the trend of sediment waves is assumed rather than demonstrated from the bathymetric grid. A white-filled circle marks the upstream end of the longitudinal profiles of channel gradient and levee relief in Fig. 6B.

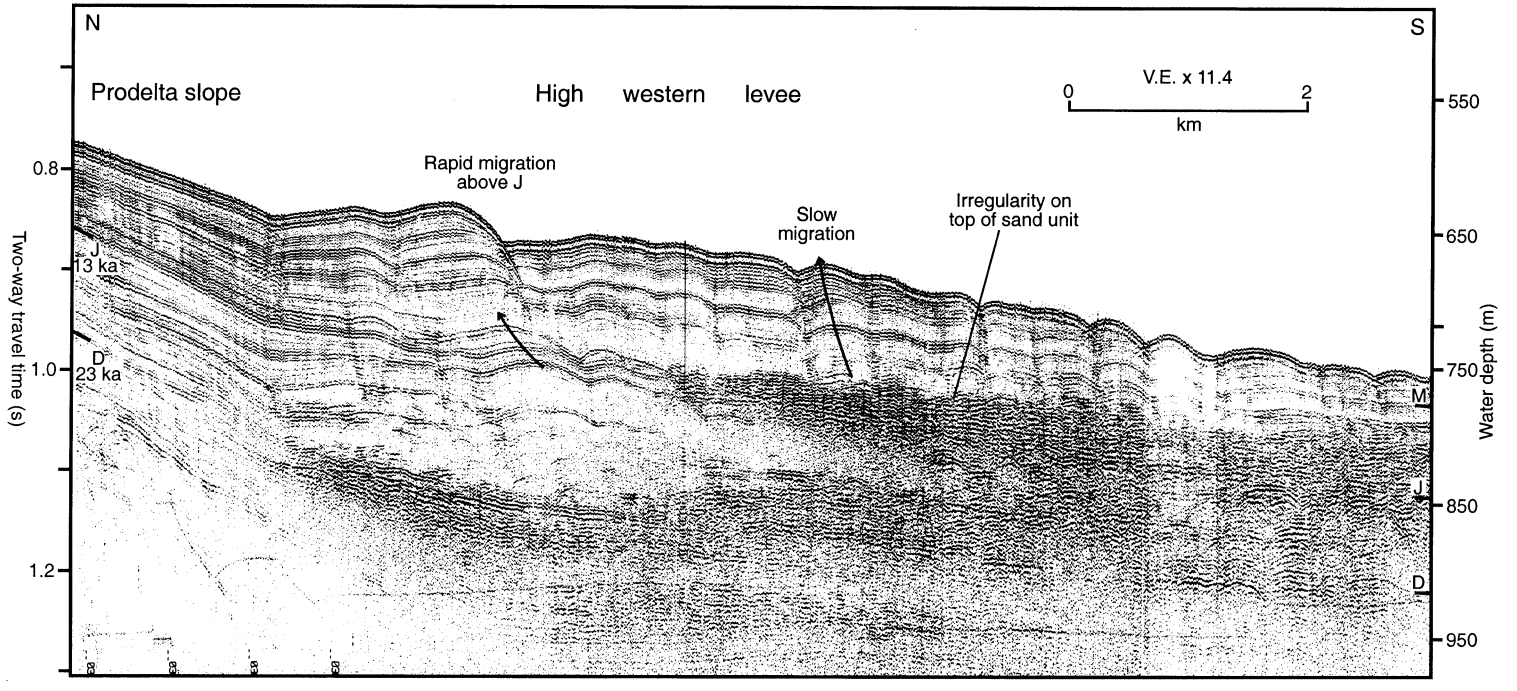

Fig. 9. High-resolution airgun seismic-reflection profile down the western levee of Hueneme Fan valley showing sediment waves prograded across mid-fan sand facies. Chronology and stratigraphic nomenclature from Piper and Normark (2001) and summarised in Fig. 8. Profile located in Fig. 7.

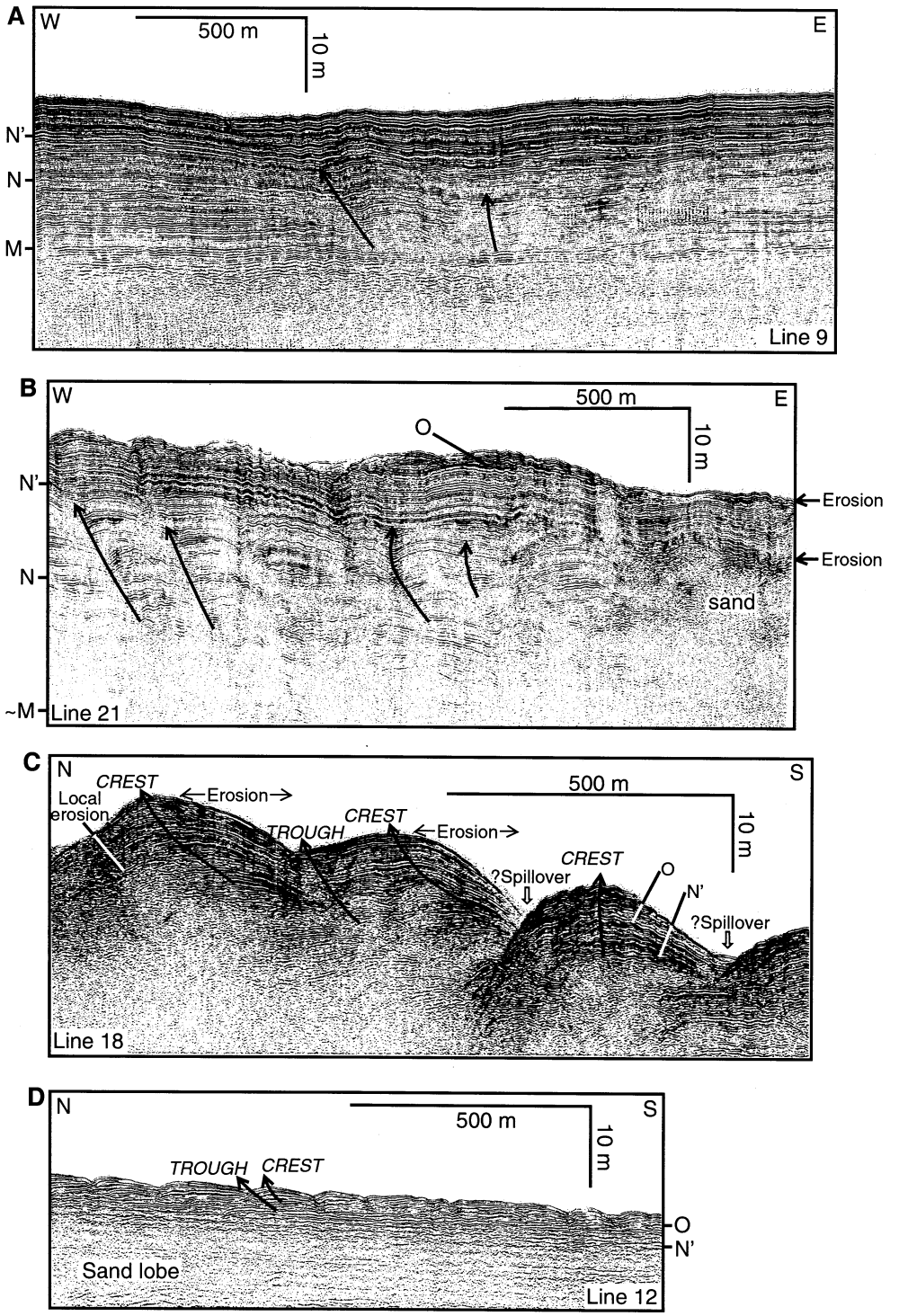

Fig. 10. Examples of deep-tow boomer profiles of sediment waves on Hueneme Fan. Profiles located in Fig. 7. Arrows show migration of sediment waves. Stratigraphic nomenclature summarised in Fig. 8.

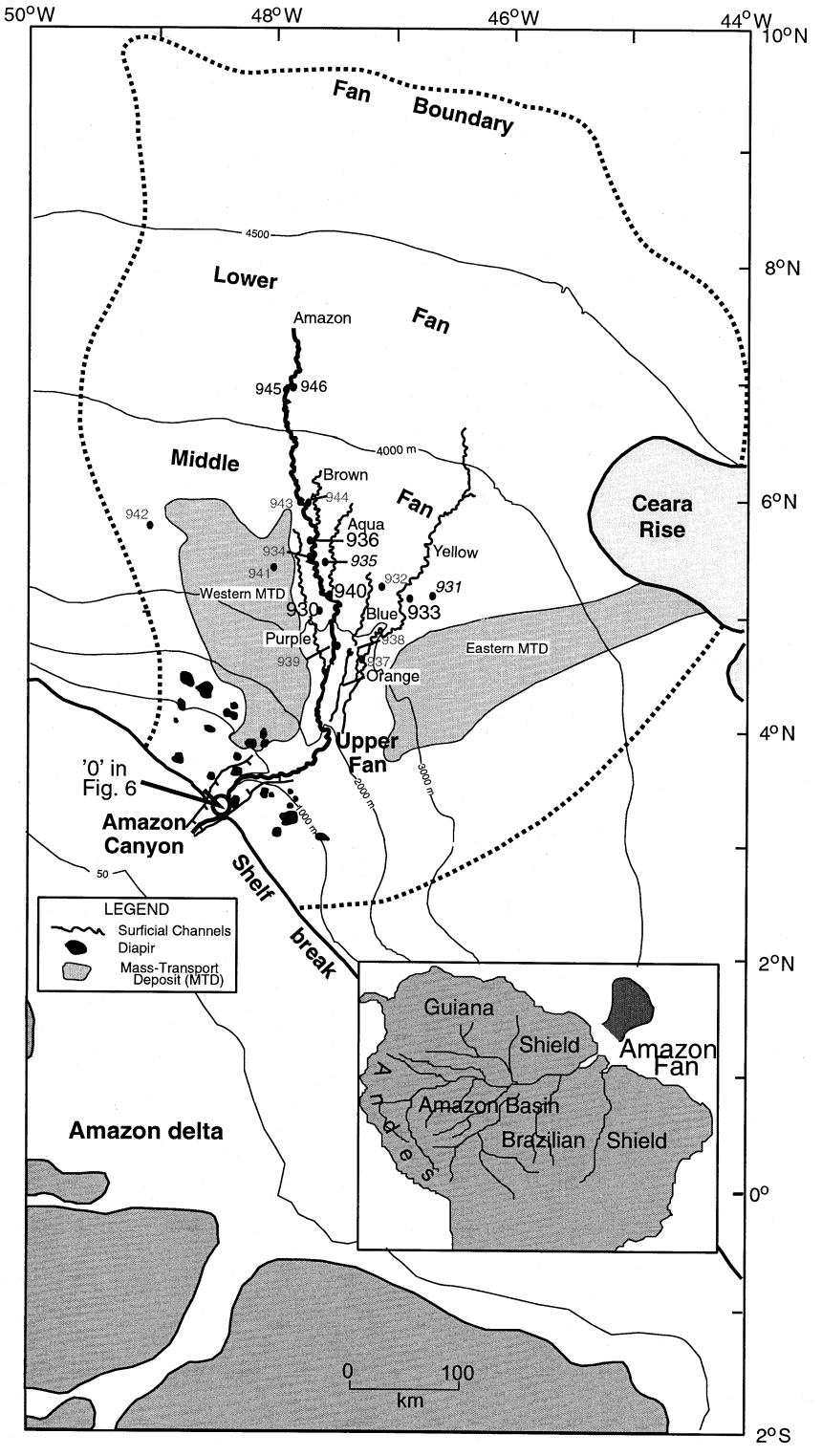
50°W
48°W
46°W
44°W
10°N
8°N
6°N
4°N
2°N
0°
2°S
Fan Boundary
4500
Lower Fan
Amazon
945
946
4000 m
Middle Fan
Brown
943
944
942
Aqua
936
934
935
Yellow
941
932
931
Western MTD
940
930
Blue
933
Purple
938
939
937
Orange
Eastern MTD
Ceara Rise
Upper Fan
3000 m
2000 m
1000 m
'0' in Fig. 6
Amazon Canyon
50
Shelf break
LEGEND
Surficial Channels
Diapir
Mass-Transport Deposit (MTD)
Guiana Shield
Amazon Fan
Amazon Basin
Brazilian Shield
Andes
Amazon delta
0
100
km

Fig. 11. Index map of Amazon Fan showing location of ODP Sites (in bold larger font) for which sediment logs are shown in Fig. 14. ODP sites also referred to in the text are shown in lower case, bold, italic font. Channel names (Amazon, Brown, Aqua, Purple, Blue, Yellow and Orange) are in order of increasing age. Figure compiled from Damuth and Flood (1985), Pirmez and Flood (1995), and Shipboard Scientific Party (1995c). A white-filled circle marks the upstream end of the longitudinal profiles of valley and channel gradients, channel width, and levee relief in Fig. 6C.

Orange in order of increasing age; Damuth and Flood, 1985). These channels have periodically shifted by avulsion across the levee.

Interpretation of 3.5-kHz profiles (Fig. 12; Pirmez, 1994) shows that sediment waves are developed on some levees of Amazon Fan, in particular between 2800 and 4000 m water depth on the associated levee crest of the Amazon Channel (Fig. 12). Sediment waves are absent on the upper fan and from 3000 to 3500 m are of very low relief (Fig. 13). The most prominent waves, from 3500 to 4000 m water depth, show a wavelength of typically 1–1.2 km and a maximum height of 20 m, tending to decrease in relief away from the channel. Levee relief above the channel floor ranges from 80 to 50 m (Fig. 6C), but sediment waves were not observed on the levees outside of the 2875–4025-m thalweg-depth range where the channel relief is either greater than 80 m or less than about 50 m. At water depths greater than 4000 m, both acoustic profiles and ODP drilling show a much higher sand content of the levees. The spatial distribution of sediment waves and wave trends cannot be mapped precisely with available spacing of 3.5-kHz profiles and neither do the GLORIA and SeaBeam images resolve the spatial orientation of these relatively low-relief sediment waves. Hiscott et al. (1997) found no evidence that overspilling flows accelerate across the levees, despite the increase in gradient compared with the down-channel gradient. They suggested that successive flows show only small variations in characteristics and represent a delicate balance between entrainment and overspill, with fine sand spilling out generally only from topographic lows along the levee system.

Several ODP holes were drilled in levee sequences showing sediment waves in 3.5-kHz profiles (Flood et al., 1995) in water depths of 3000–3500 m, where mean wavelengths are typically 400–700 m and wave heights <5 m. Unfortunately, the waves are not visible in the rather low-resolution seismic-reflection profiles available from the fan and 3.5-kHz profiles rarely image well below 30 mbsf[1].

Hole 930B is located on the down-current side of the wave, close to the trough (Fig. 13A). Hole 930D is located near the crest of the next wave. Progressive increase in wave height has taken place above an almost planar reflection near the limit of 3.5-kHz acoustic penetration that projects at about 35 mbsf at Hole 930B (Fig. 13A). Sediment waves 2 km to the south (Fig. 13B) have a rather thicker section and show three phases of growth: (1) increase in crest height and migration in an upper section corresponding to mud turbidites from 2 to 6 mbsf and overlying hemipelagic deposits in Hole 930B (Fig. 14); (2) a more uniform drape in the interval from 6 to 11 mbsf, where bioturbated muds are found in 930B; (3) and then an interval from 11 to 32 mbsf of even greater crest growth and migration than in the 0–6 m interval, corresponding to mud with sand and silt beds in 930B. Hole 930B, close to the trough, has a thinner overall section (Fig. 14) and thinner individual beds (Fig. 15) compared with Hole 930D on the up-current flank near the crest (Table 1). Some individual sand beds can be correlated across the $\sim$200 m offset between holes, whereas other sand beds pinch out to thin silt laminae. Maximum sand bed thickness is 2.5 cm (Fig. 15; Table 1). Stratigraphic correlation implies that the upper $\sim$32 mbsf were derived from the Amazon Channel 8 km to the east and the underlying interval from the now abandoned Purple Channel 15 km to the west.

Site 933 is located on the down-current side of a sediment wave, about half-way between trough and crest (Fig. 13C). The upper 14 m of colour-banded and bioturbated mud (Fig. 14) forms a

[1] mbsf = metres below sea floor.

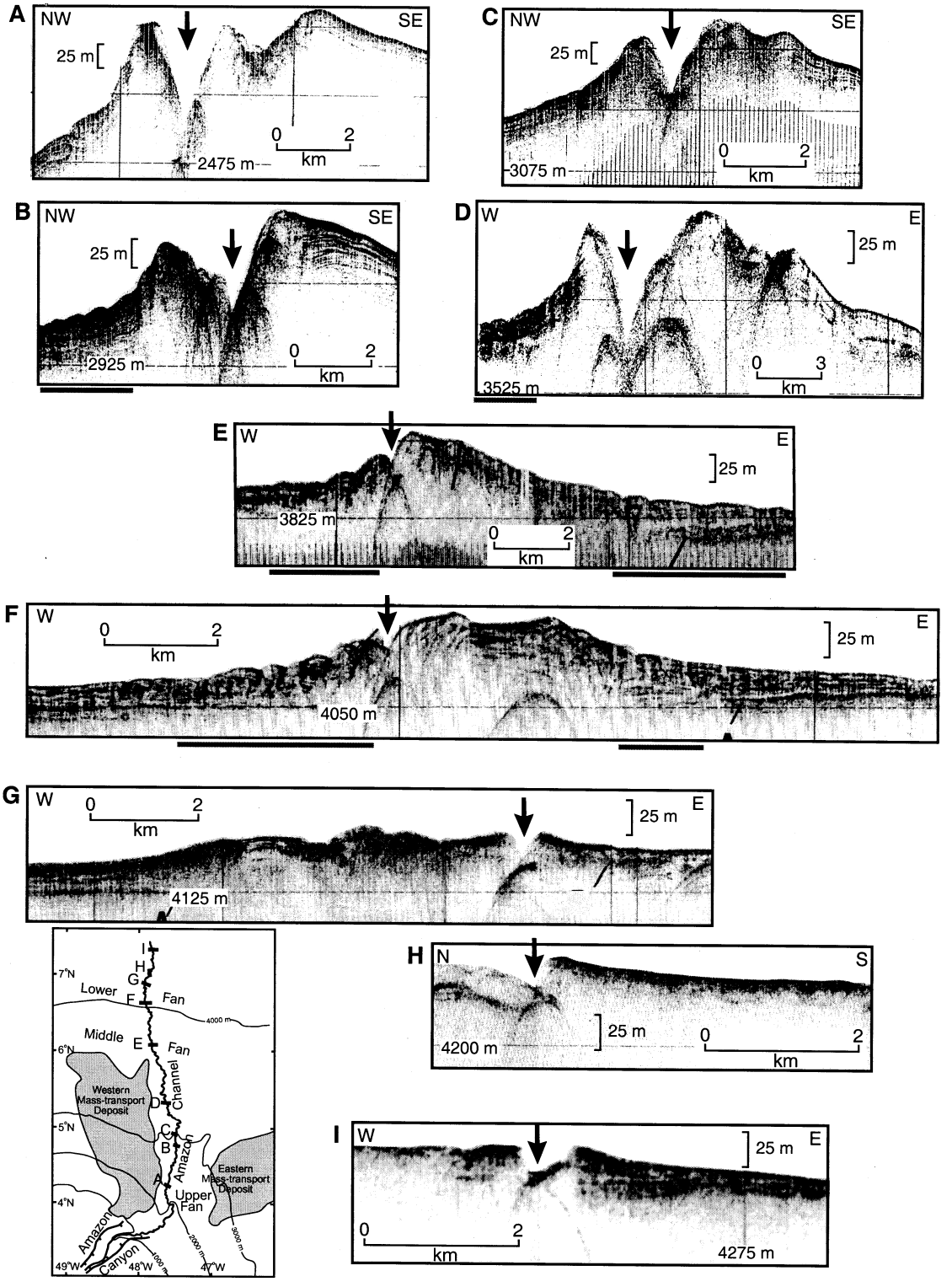
A
NW
SE
25 m
0
2
km
2475 m
C
NW
SE
25 m
0
2
km
3075 m
B
NW
SE
25 m
2925 m
0
2
km
D
W
E
25 m
0
3
km
3525 m
E
W
E
25 m
3825 m
0
2
km
F
W
0
2
km
E
25 m
4050 m
G
W
0
2
km
E
25 m
4125 m
H
N
S
25 m
4200 m
0
2
km
I
W
E
25 m
0
2
km
4275 m
I
H
G
F
E
D
C
B
A
Lower
Fan
Middle
Fan
Channel
Amazon
Upper
Fan
Western
Mass-transport
Deposit
Eastern
Mass-transport
Deposit
Amazon
Canyon
7°N
6°N
5°N
4°N
49°W
48°W
47°W
4000 m
3000 m
2000 m
1000 m

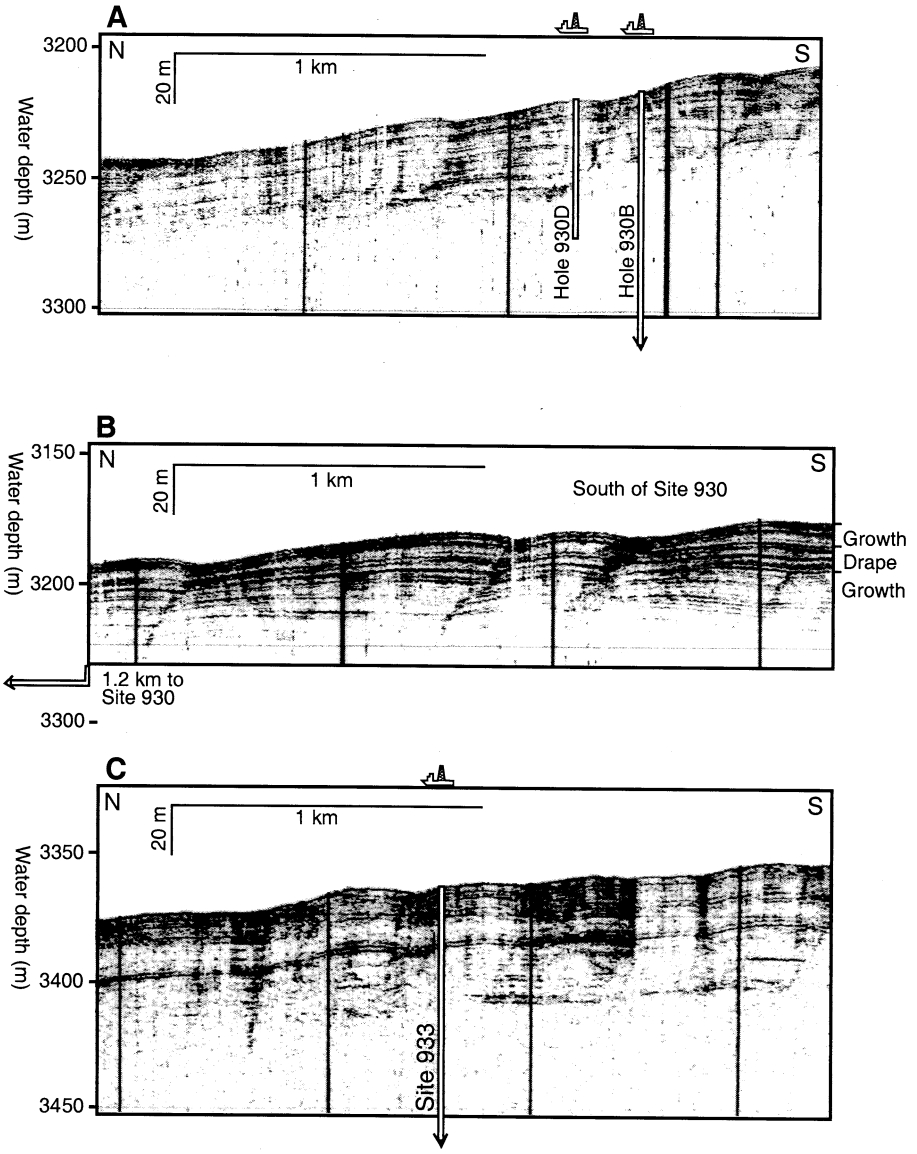

Fig. 13. High-resolution 3.5-kHz profiles of sediment waves on Amazon Fan. (A) Site 930; (B) 2 km south of Site 930; (C) Site 933. Modified from Shipboard Scientific Party, 1995a,b. Note there is an error in Fig. 3 of Shipboard Scientific Party (1995a). We have corrected the position of Holes 930B and 930D to reflect the position data presented at the beginning of the Site 930 chapter.

Fig. 12. High-resolution 3.5-kHz profiles illustrating the morphological changes on the levees of Amazon Channel. Sediment waves are generally absent or very low relief on the upper part of the fan (A–D), show highest relief on the middle fan (profiles E and F), and are absent on lower part of the fan (profiles G–I). Lower fan profiles indicate a marked change in the acoustic facies of the levees consistent with an increase in sand content. Arrow at the top of each profile marks the axis of Amazon Channel. Dashed grey line below each profile denotes the extent of sediment waves. Depth marks in each profile are in metres below sea level.

Table 1
Sediment wave bed data (Amazon Fan, ODP Leg 155)

	Hole 930B	Hole 930D	Hole 933A	Hole 936
Wave interval in hole	9.8–43.7 mbsf	13.5–51.5 mbsf	13.47–58.91 mbsf	8.32–40.29 mbsf
Thickness of sediment wave interval	32.2 m	36.9 m	45.44 m	31.97 m
Number of silt laminae	312	289	351	145
Number of silt/sand beds	17	62	147	51
Total number of beds and laminae	329	351	498	196
Sum of silt/sand bed thicknesses	36 cm	122 cm	313.5 cm	96 cm
Number of beds with sand	>3	>25	>93	0
Position of hole with respect to wave form	Just upflow of trough	Just upflow of crest	Just upflow of trough	Crest of wave*
Number of beds (total) per meter	10.22	9.51	10.96	4.54*

drape which was probably derived from the Amazon Channel more than 25 km distant. The underlying 55 m of section was deposited on the right-hand levee of the 'Yellow' channel, about 4 km from the channel axis (Fig. 11) at a time when the Brown and Aqua channels were active. The thickening of strata towards the Yellow channel demonstrates that sedimentation was related to this formerly active channel, that may have captured and rechannelised flow overbanking from the Amazon Channel system (Piper et al., 1997). The sediment section is remarkably similar to that at Site 930 (Table 1), with tentative correlations shown between slumped intervals and particularly thick sand beds (Fig. 14).

Site 930, on the left side of the Amazon Channel, and Site 933, on the right side of the Yellow Channel, show correlative variations in the abundance of sand and silt beds with the section at Site 940 near the crest of the right hand levee of the Amazon Channel (Figs. 11 and 14). This variation in sand and silt abundance over a wide range of bathymetric settings suggests that it reflects variations in the thickness and/or sediment load of turbidity currents derived from the Amazon delta. The detailed correlations between Site 933 and Site 930, 80 km distant, indicate that individual turbidity currents that formed sediment waves flow across extensive overbank areas on both sides of the channel.

In contrast to the Monterey and Hueneme fans, which have gently arcuate channels with a prominent right-hand levee, the Amazon Fan sediment waves are formed on levees of highly sinuous channels in what is commonly considered a muddy turbidite system. The composition of sediment within the sediment waves, together with the stratigraphic control provided by ODP core data from Amazon Fan, confirm that in up-flow-migrating sediment waves more and thicker sand and silt beds were deposited on the up-current flank of the waves. In addition, the coring results suggest that most of the turbidity current overflows in the area of the sediment waves on Amazon Channel were probably less than 50 m thick.

2.4. Deep-water Niger delta

Extensive leveed channel deposition characterises the late Pleistocene section in the deep-water environment offshore eastern Nigeria (Skaloud and Cassidy, 1999; Posamentier and Kolla, in press). These channels display complex cut-and-fill morphology suggesting a multistage evolution. Levee thicknesses of 110–120 m and widths of 10–12 km characterise these systems (Fig. 16). Levee

Fig. 14. Generalised stratigraphic columns through sediment wave facies. Columns 930B, 933, and 940A from Flood et al., 1995; Column 930D constructed from visual core description logs from ODP Leg 155. See also Table 1. Stratigraphic correlation is based on Piper et al. (1997). Heavy dashed lines show depositional intervals corresponding to the Purple, Aqua, and Brown channel activity.

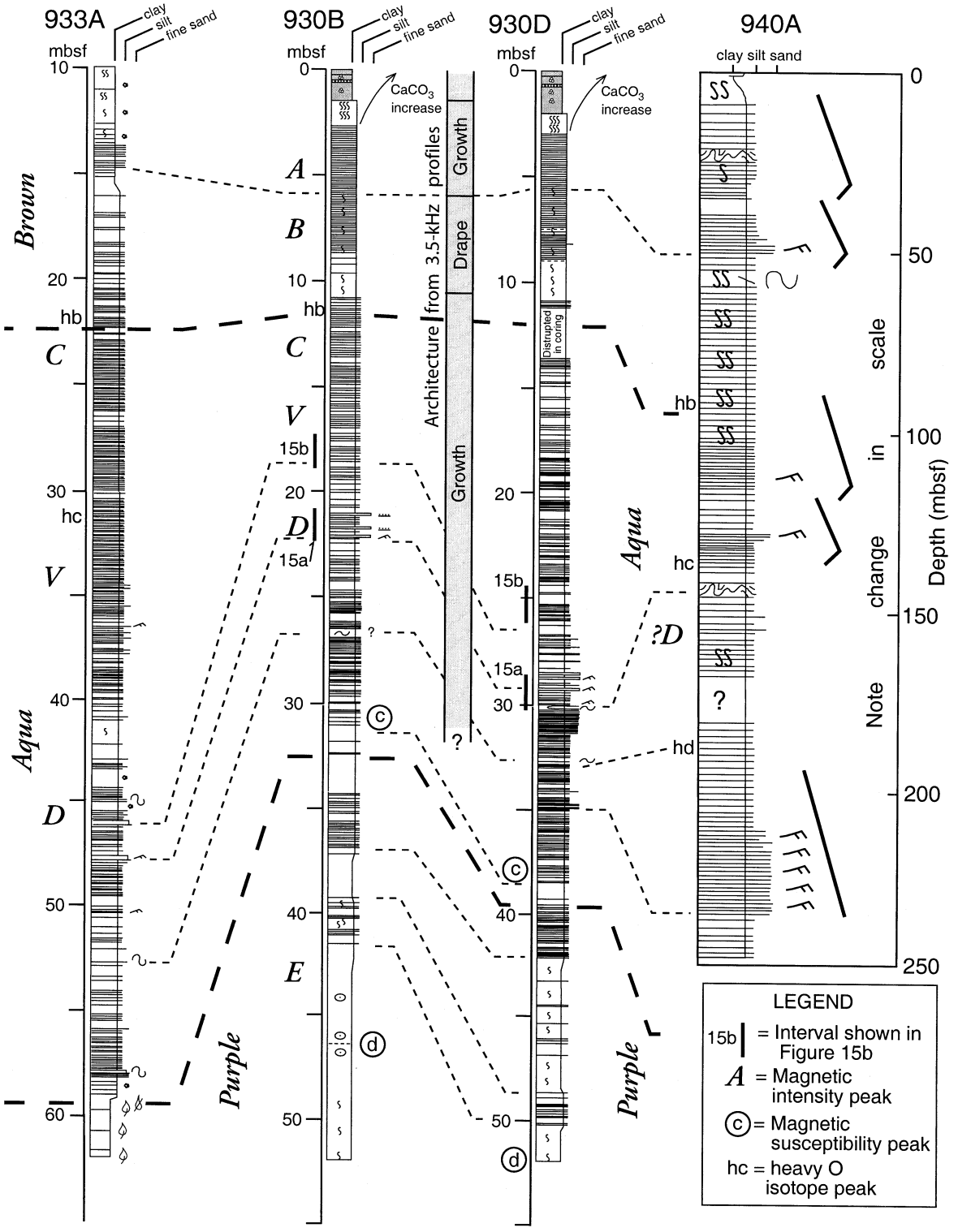
933A
930B
930D
940A
clay
silt
fine sand
clay silt sand
mbsf
Brown
Aqua
Purple
hb
hc
hd
A
B
C
D
E
V
15a
15b
?D
?
CaCO3 increase
Architecture from 3.5-kHz profiles
Growth
Drape
Growth
Disrupted in coring
Note change in scale
Depth (mbsf)
LEGEND
15b = Interval shown in Figure 15b
A = Magnetic intensity peak
c = Magnetic susceptibility peak
hc = heavy O isotope peak

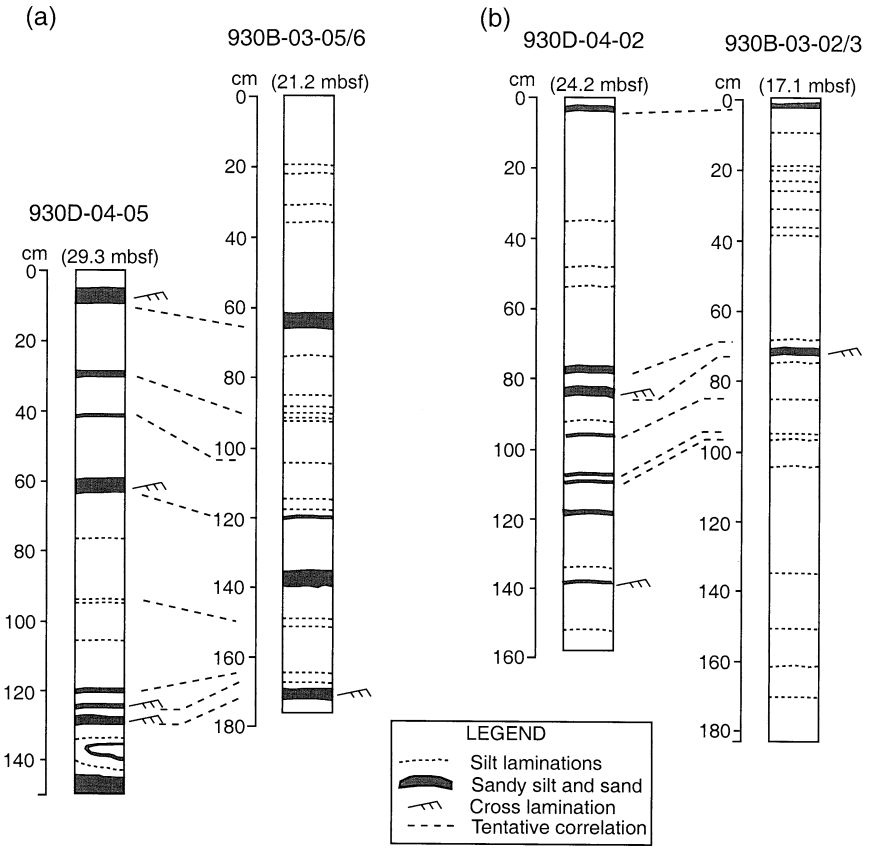

Fig. 15. Detailed sediment logs constructed from visual core description logs from ODP Leg 155 drilling on Amazon Fan showing representative intervals to illustrate lithology and correlation within the sediment wave sequence. The basis of the correlation is shown in Fig. 14. Relative position of the ODP holes is shown in Fig. 13.

dimensions are relatively symmetrical on either side of the channel complex; the Coriolis force is negligible in this area, given the proximity to the equator.

Sediment waves characterise more than 100-m thickness of section in the overbank environment. These features are arcuate to linear in planform and are oriented oblique to the channel within 1 km of the channel, but then bend to be almost orthogonal to the general channel trend (Fig. 17). The long axes of these sediment waves range in length from 3 to 7 km. Wavelengths range from 0.6 to 1.0 km and wave heights from 15 to 30 m (Fig. 18). The waves show strong up-current migration, with the migration-to-aggradation ratio increasing upwards (in contrast to Hueneme Fan). This geometry rules out rotational slumping (with concave-up slide planes) as the mode of formation for these features.

2.5. Makassar Strait

A well-developed (?)mid-Pleistocene symmetrical leveed channel system (Fig. 19) in the Makassar Strait area offshore eastern Borneo, Kalimantan, Indonesia has levees as much as 100 m high and 4–5 km wide with extensive sediment-wave fields (Fig. 20) (Posamentier et al., 2000). This system is buried by an 80–100 ms (~65–80 m) seismically low-amplitude reflection section (Fig. 21). A moderate- to high-sinuosity leveed channel flowing from west to east is clearly imaged. Linear

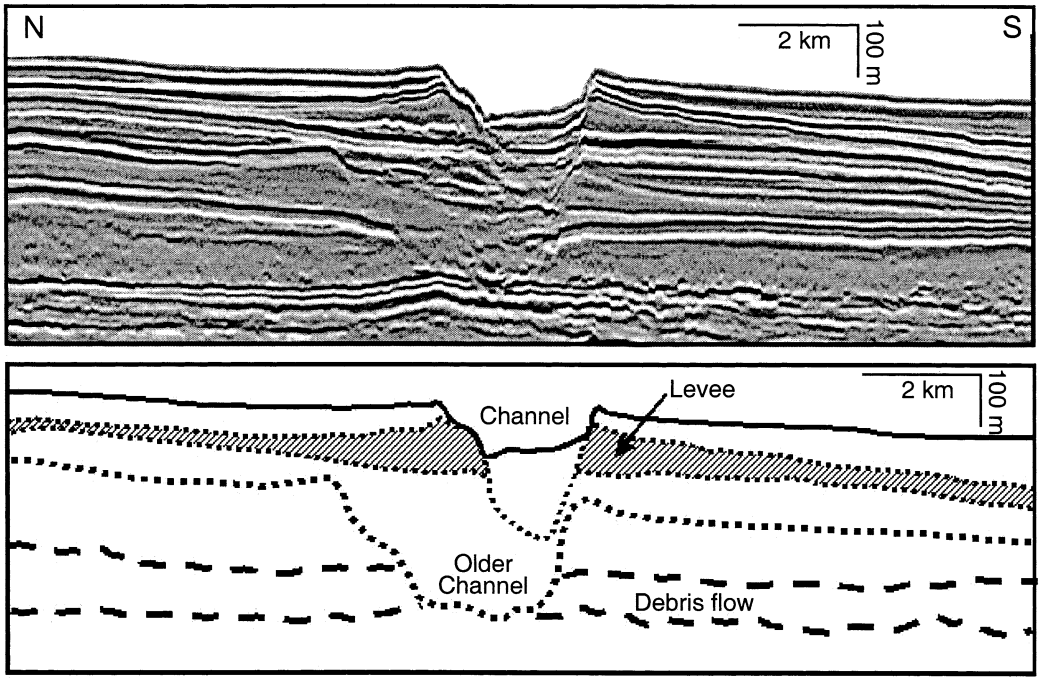

Fig. 16. Seismic-reflection profile oriented transverse to a high-sinuosity leveed channel in deep-water offshore Nigeria. The levees thin from 110–120 m to less than 5 m over a distance of 10–12 km away from the margins of the channel.

to slightly arcuate features on either side of the channel are interpreted to be sediment waves (Figs. 20 and 22). Two families of sediment waves can be observed on the right-hand levee, but the reason for this complexity is uncertain. On the left-hand levee, the planform of the waves is subparallel to the channel and arcuate about the outer bends of meanders (Fig. 22). Sediment waves are best developed on outer bends that are abrupt and would have overbank flow parallel to the regional gradient. The area with high wave heights covers 3–6 km^2. On bends where overbank flow would be against the regional gradient, sediment waves do not form. The long axes of these sediment waves range in length from 0.3 to 2.0 km, with wavelengths of 0.2–0.5 km and wave heights of 10–20 m that progressively diminish with distance from the levee crest (Fig. 21). Wavelength increases non-uniformly. By analogy with the Shepard meander on Monterey Fan, it would be this area where the best turbidite sand bed development would be expected.

2.6. Reserve Fan

Reserve Fan is a small fan that developed from the hyperpycnal discharge of mine tailings into Lake Superior (Normark and Dickson, 1976a,b). The fan, which has developed basinward of a steep prodelta slope that extends to about 180 m depth, has two leveed channels about 5 km in length (Fig. 23A). Turbidity-current flow through the larger channel was monitored (Normark, 1989) and showed that flow thickness (based on a measure of sediment concentration with depth in the flow) was 16 m thick over a 4-m-deep channel; flow velocity was 0.1 m/s (Fig. 23C). Overbank flow episodes from the smaller (in cross section) eastern channel on Reserve Fan have been measured with velocities as high as 0.2 m/s at a depth equivalent to 14 m above the adjacent channel floor. Closely spaced (35-m grid) high-resolution seismic-reflection profiles show that sediment waves are developed on the levees (Fig. 23B).

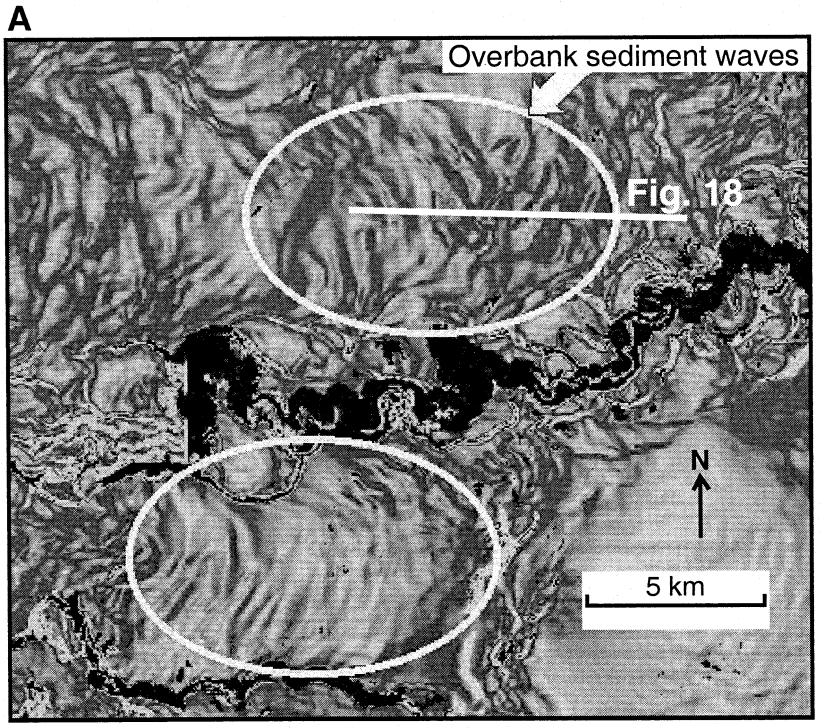
A
Overbank sediment waves
Fig. 18
N
5 km

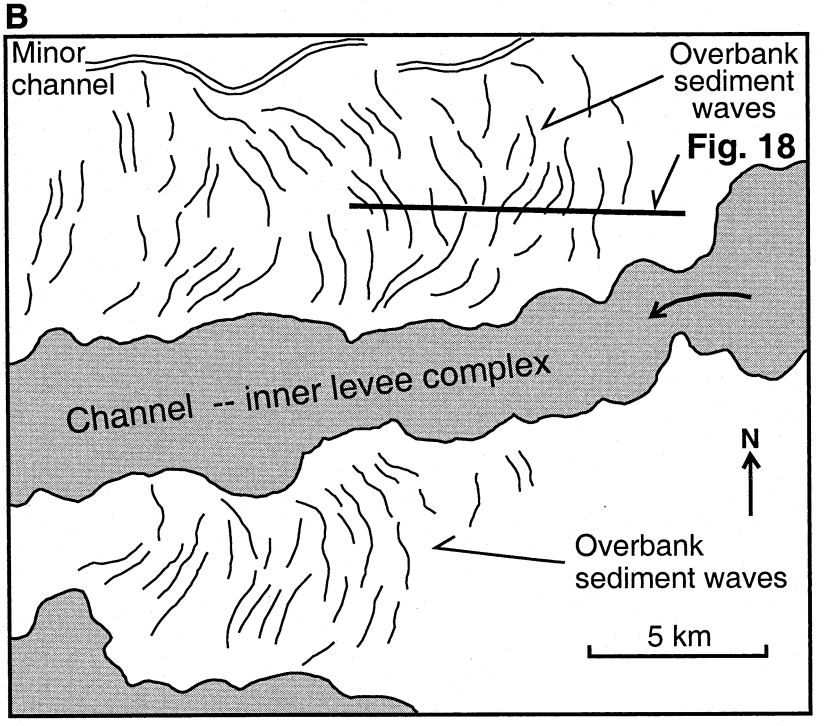
B
Minor channel
Overbank sediment waves
Fig. 18
Channel -- inner levee complex
N
Overbank sediment waves
5 km

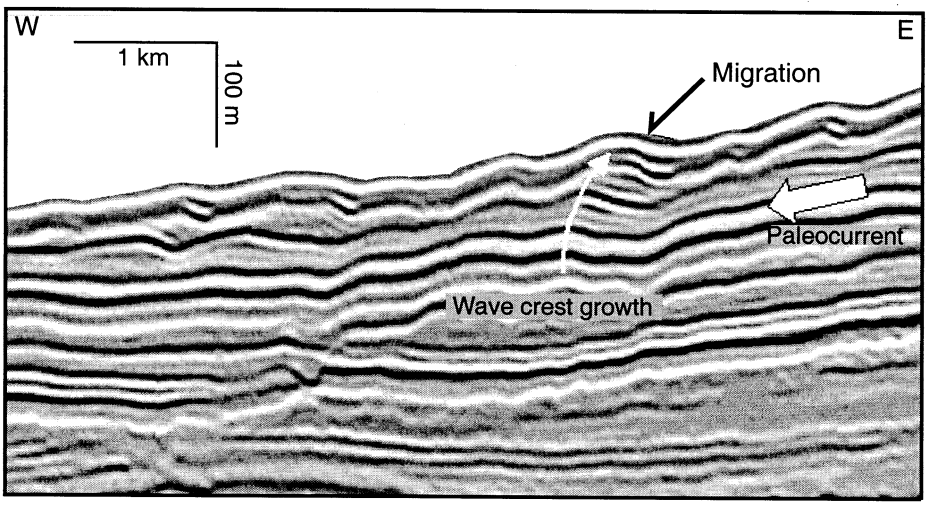

Fig. 18. Seismic-reflection profile oriented normal to the long axes of sediment waves, offshore Nigeria. Slight thickening of the up-system flanks of these waves can be observed suggesting accretion on that side, forming a migration wave. Location of profile shown in Fig. 17.

3. Discussion

3.1. Controls on the scale of turbidite sediment waves

We use information on the mean dimensions of turbidite sediment-wave fields to investigate scaling relationships between sediment waves and other characteristics of turbidite systems such as channel size and regional and channel gradients. Data on dimensions plotted in Fig. 24 are of variable quality, because only a few wave fields have swath-bathymetric, sidescan-sonar, or 3D seismic-reflection data that accurately define the trend of waves. Most wavelengths are estimated from seismic-reflection sections inferred to be approximately orthogonal to waves, but if the sections are more than 30° oblique, the wavelength may be significantly overestimated. Wave forms die out along strike (Figs. 3, 17 and 22), so that the total number of sediment waves in any particular length of seismic-reflection section depends on the precise location of that section.

In general, length and height of fine-grained turbidite sediment waves show a positive correlation (Fig. 24A and Table 2). The size of sediment waves shows much scatter when compared with channel cross-sectional area or width (Fig. 24B), suggesting that any relationship to the size of turbidity currents in a turbidite system is quite complex, although smaller waves tend to occur adjacent to smaller channels (e.g. inner Hueneme levee, Reserve Fan). There is a tendency for larger waves to occur on lower regional gradients (Fig. 24C), but as discussed below, this relationship may not imply any causal relationship because the distribution of sand beds on levees suggests that greater spillover tends to occur on lower gradients. The smallest waves, however, also occur more distally on the fans (e.g. Monterey Fan: Fig. 1; lower Hueneme Fan: Fig. 10D). In a general manner, in areas where there is evidence for thicker overbanking flows, the wavelength and height of sediment waves are greater. Thick overflows can result from a very local channel morphology, where the action of the centrifugal force

Fig. 17. (A) Map of dip magnitude derived from seismic-reflection data of the sea floor in deep-water offshore Nigeria. Dips of up to 10° characterise the flanks of these waves. (B) Schematic map showing trend of sediment waves with respect to the channel–inner levee complex. Location of seismic-reflection profile in Fig. 18 is shown.

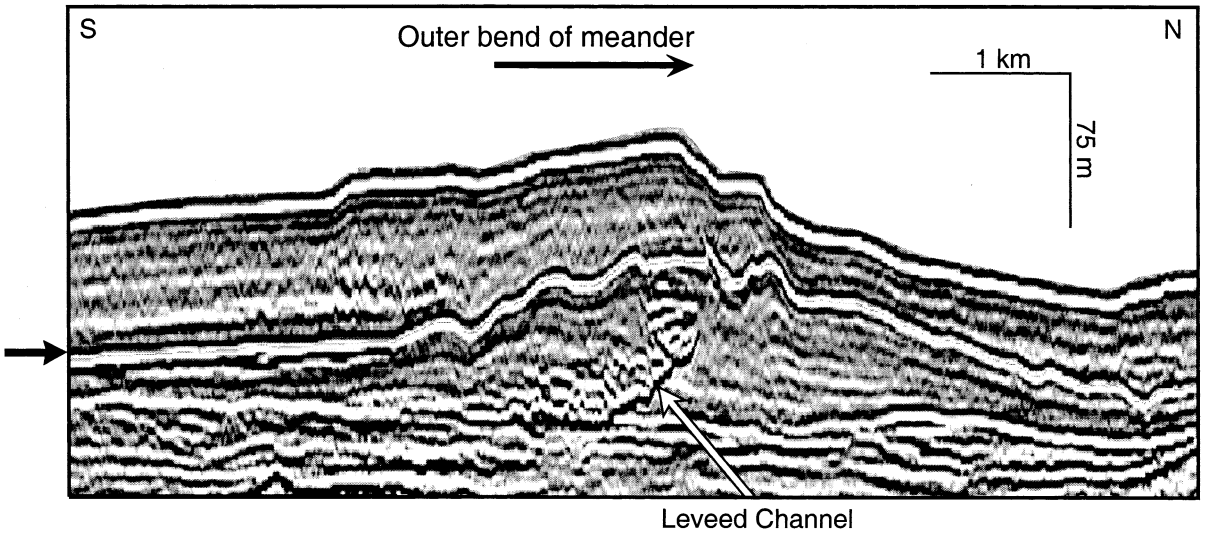

Fig. 19. Seismic-reflection profile transverse to a well-developed mid-(?)Pleistocene leveed channel, in Makassar Strait, Kalimantan, Indonesia. Bold arrow at left margin shows horizon depicted in Fig. 20. Location of profile shown in Fig. 20.

increases dramatically, such as at sharp bends in channels or in meanders. For example, thick flows on the outer bend of the Shepard meander on Monterey Fan correlate with unusually large sediment waves on that reach of the channel (McHugh and Ryan, 2000). Thick overflows also occur where channelised turbidity currents exceed the local channel depth. Relative flow thickness in relation to levee height increases rapidly downchannel as flow thickness increases because of water entrainment. Modelling of flows on the Var Fan valley (Piper and Savoye, 1993) suggests that flows thicken considerably down the middle fan valley, concomitant with a decrease in elevation of the levee (Var Sedimentary Ridge) and an increase of the wavelengths of sediment waves (Migeon et al., 2000). On Amazon Fan, levee sediment becomes progressively coarser grained down the Amazon Channel system, probably implying progressively greater thickness of spillover turbidity currents (Hiscott et al., 1997) in relation to a decrease in levee relief. In general, the wavelength of sediment waves on Amazon Fan is greater near the 4000-m isobath than near the 3000-m isobath. These observations suggest that sediment waves are always correlated with areas of high sediment supply that is necessary to allow sediment-wave initation and migration (Migeon et al., 2000). Overflow thickness and sediment supply are both constrained by the levee relief and channel morphology, which are therefore important factors influencing the size of sediment waves.

The two numerical analyses of flow conditions by Normark et al. (1980) and Flood (1988) both require a densiometric Froude number close to 1 and Normark et al. (1980) require a substantial flow thickness for the turbidity current. Such conditions are supported by observations on Reserve Fan. Flow thicknesses are known to be at least 16 m on the middle fan over a 4-m-deep channel (Fig. 23C), suggesting an overbank flow about 12 m thick (Normark, 1989). The Froude numbers are estimated as 1.5. Nearby sediment waves on a gradient of 0.02 have a wavelength of about 120 m. Application of the numerical model of Normark et al. (1980) implies an overbank flow thickness of about 12 m, similar to flow thickness estimated from the vertical concentration of magnetite grains (sampled at half-metre intervals) in the flow. The longer wavelength sediment waves on the lower fan would be consistent with flow thickening by entrainment.

Application of the numerical model of Normark et al. (1980) gives estimates of flow thick-

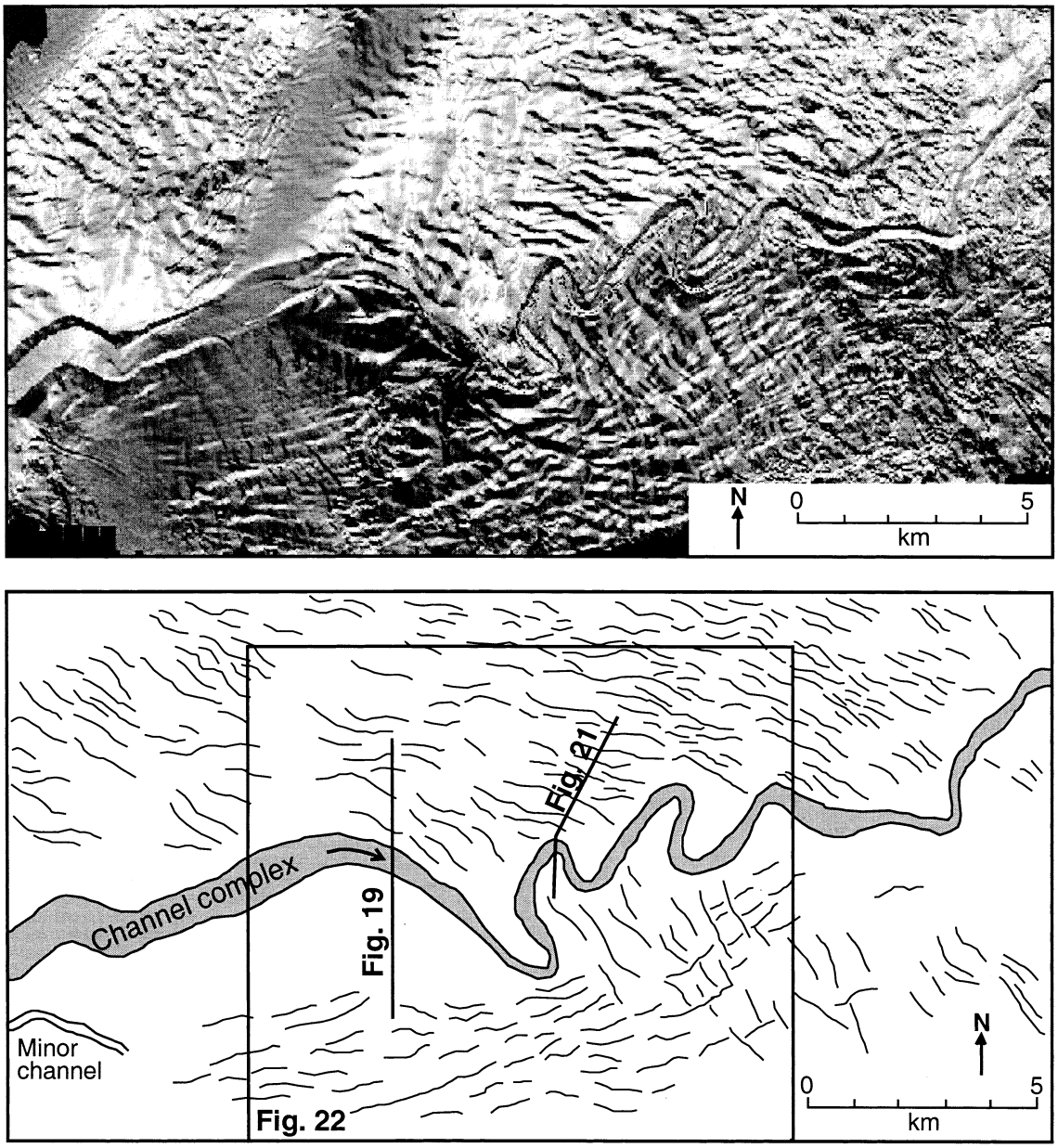

Fig. 20. (A) Pseudo-3D relief map (based on azimuth of dips derived from seismic-reflection data) of the surface identified in Fig. 19. (B) Schematic map showing trend of sediment waves with respect to the channel complex. Locations of seismic-reflection profiles in Figs. 19 and 21 are shown. Box outlines area of Fig. 22.

ness on Amazon Fan of about 100 m (e.g. for the sediment waves at Site 930 where the regional gradient is 0.01). The very thin turbidite sections on old levee crests in the uppermost parts of Sites 931 and 933, located some 50 m above the regional seafloor, suggest that although a few flows may have been as much as 100 m thick, most flows were <50 m thick. Hiscott et al. (1997) argued that overbanking flows from Amazon Channel could be as thin as 5 m and that very thick flows

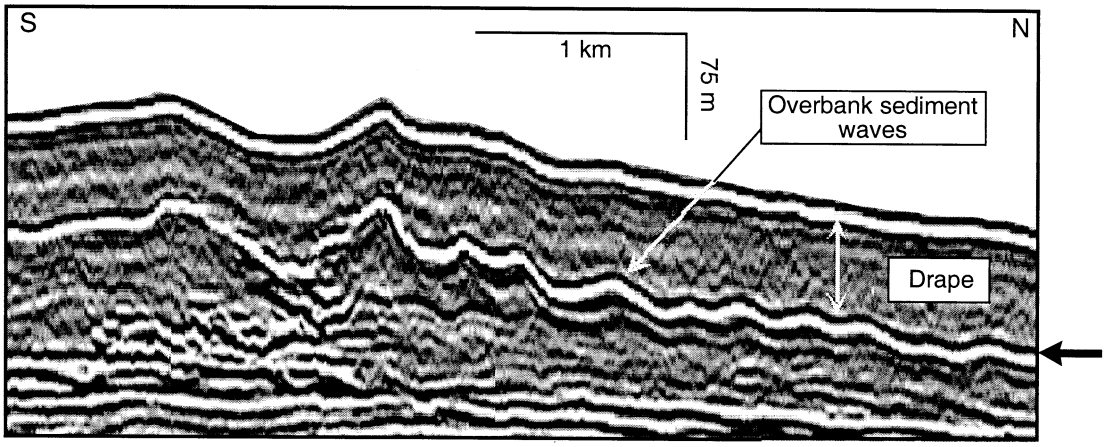

Fig. 21. Seismic-reflection profile oriented normal to long axes of overbank sediment waves offshore Kalimantan, Indonesia. Sediment waves are observed within as well as at the top of the levee. Note the sediment-wave height decreases with distance away from the levee crest. Location of profile shown in Fig. 20.

were unlikely except at saddles in the levees because of the great continuity of the channel-levee system. On the other hand, the great extent of some turbidite beds (Figs. 14 and 15) requires flows that travel many tens of kilometres overbank and are thus probably a few tens of metres thick. Overbanking flows would presumably thicken by entrainment as they crossed the steep levee.

Overbank flows 100–150 m thick, estimated independently from numerical models, are thought to be responsible for sediment-wave construction on the distal part of the Var Sedimentary Ridge (Migeon et al., 2001). On Hueneme Fan, flow thickness can be estimated from the fact that the larger sediment waves above horizon N′ (Fig. 10C) are in an area where flows deposited turbidite silt or mud over the crest of a levee 40 m above the channel floor, whereas down-fan, where waves are smaller (Fig. 10D), silt and mud turbidites extend only about 20 m up the basin flank.

It therefore appears that thicker overbanking flows are related to larger sediment waves. The Normark et al. (1980) two-layer model predicts relationships between flow thickness and wavelength of sediment waves that yield estimates of flow thickness only slightly greater than those derived from field observations. Wynn et al. (2000b) show that many sediment waves develop from flows with densiometric Froude number in the same range as cited by Allen (1984) for the formation of antidunes (0.85–1.7), suggesting that their absence in distal parts of turbidite systems may result from the low Froude number expected there. This is consistent with the observation that sediment waves on the backsides of levees commonly migrate up-flow.

It is, however, not clear that high Froude numbers in every flow are essential for deposition on or migration of sediment waves. Seismic-reflection profiles show that many waves are inherited from surfaces tens to hundreds of metres below the seabed. In some cases, irregularities in underlying sand deposits appear to form an initiation surface for sediment waves. On Hueneme Fan, the boomer profiles show that some sediment waves do develop on essentially planar sand surfaces. It may be that in some cases, unusually thick flows do initiate a pattern of sediment waves by a process that can be described by the numerical modelling of Normark et al. (1980) or of Blumsack and Weatherley (1989). However, for most sediment waves, the pattern of differential deposition may result from flow interaction between a relatively thin turbidity current and a pre-existing wave form (Lee et al., 2002). This process has been modelled numerically by Lee et al. (2002),

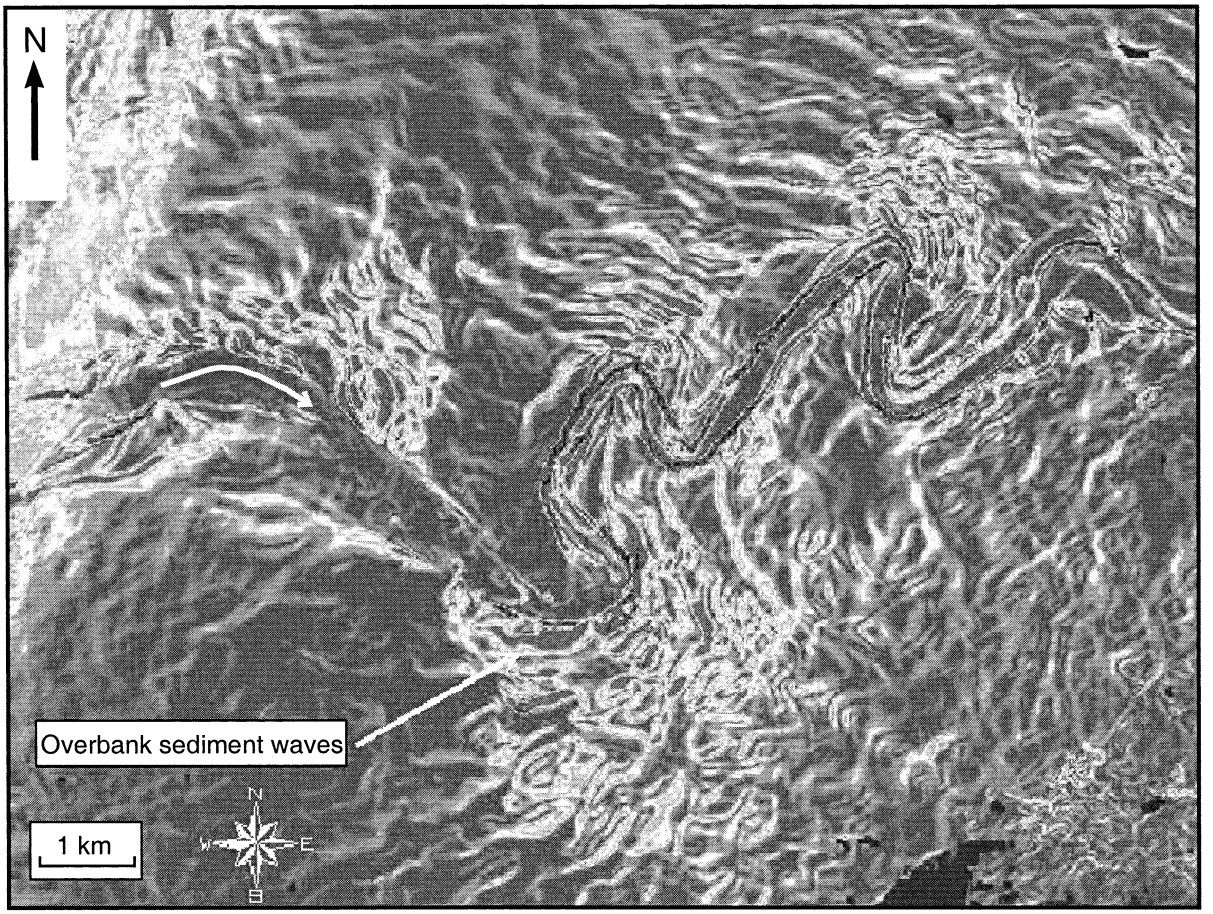

Fig. 22. Map of dip magnitude derived from seismic-reflection data illustrating largest-scale sediment waves developing in clusters or fields in close proximity to leveed-channel outer bends (see discussion in Posamentier et al., 2000). Location shown in Fig. 20.

who demonstrate that deposition takes place preferentially on the up-current side.

3.2. Near-bed flow processes

The combination of core data and high-resolution boomer seismic-reflection profiles from Hueneme Fan and 3.5-kHz profiles from Monterey and Amazon fans shows that prograding sediment waves experience preferential deposition of both sand and mud on the up-current side and less deposition or in some cases actual erosion (Fig. 10C) on the down-current side. In contrast, aggradational waves show relatively uniform sediment deposition over both up-current and down-current slopes, with minor preferential deposition on the up-current side resulting in very slow upflow migration. In some cases, this draping sediment is deposited preferentially in the troughs (Fig. 10A), resulting in decreased crest elevation.

The general distribution of sediment observed on both Monterey and Amazon fans is that on the up-current side and crests of waves, sand beds are thicker and more abundant. Similar observations are reported from the Var Fan, where grain size and sand content also decrease from the up-current side to the crest and the down-current side of a single sediment wave (Migeon et al., 2001). On Amazon Fan, some sand beds show tractional features such as ripplemarks and some silt laminae are lenticular or starved (facies 5 and 6 of Piper and Deptuck, 1997). Core data from Mon-

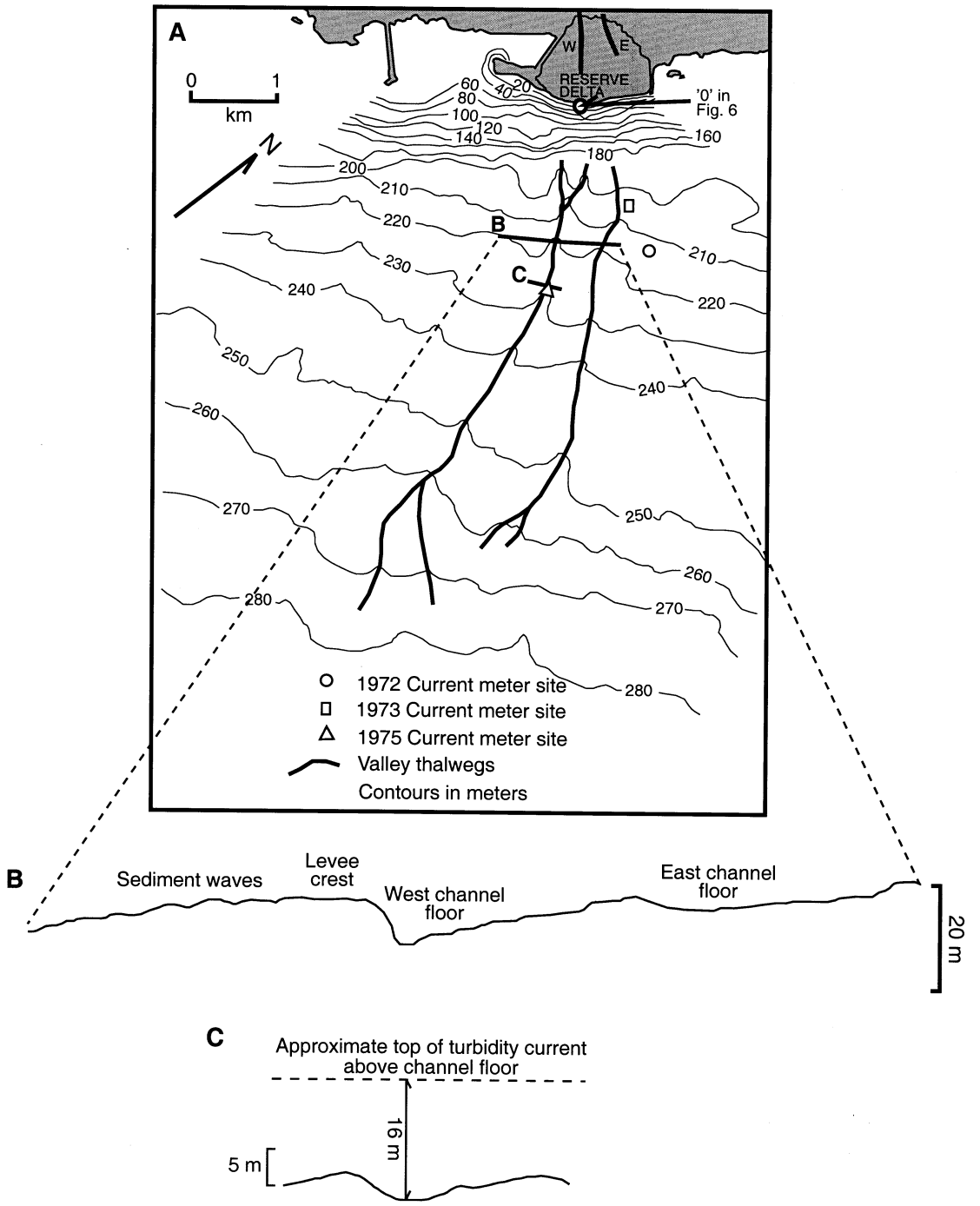

Fig. 23. Reserve Fan, Lake Superior, formed from discharge of tailings. (A) Map showing bathymetry and sites of current meters. (B) Cross section drawn from high-resolution seismic-reflection profile showing sediment waves. (C) Cross section at current meter C showing relationship of turbidity current to levees. A white-filled circle marks the upstream end of the longitudinal profile of channel gradient in Fig. 6D.

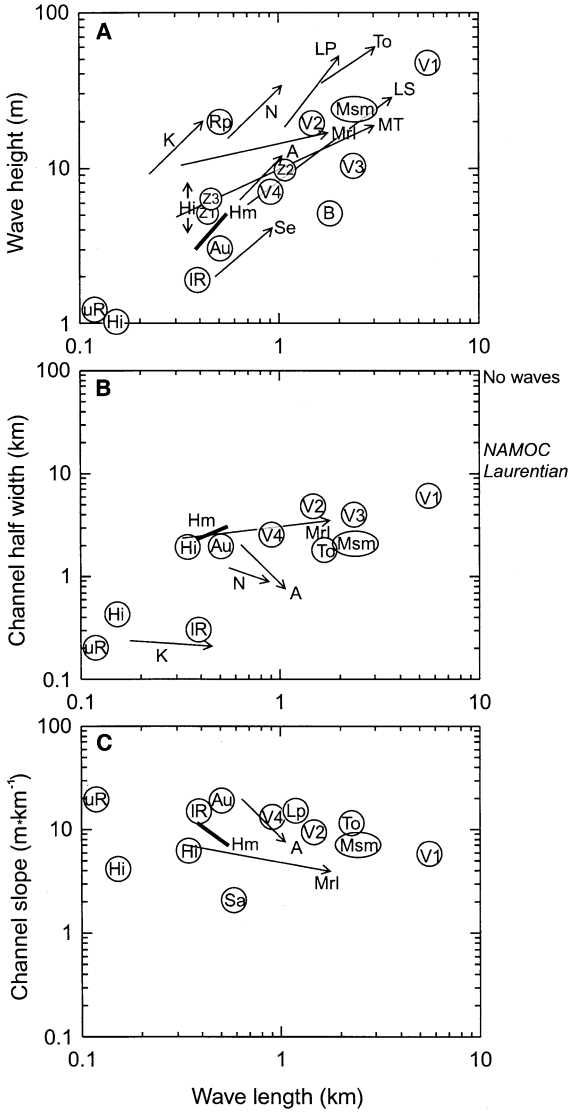

Fig. 24. (A) Cross plot of wavelength against wave height for sediment waves. (B) Plot of wavelength against channel cross-sectional area. (C) Plot of wavelength against regional gradient. A = main Amazon Channel; Au = upper Amazon Channel (Flood et al., 1995); B = Barra Fan (Howe, 1996); Hm = main Hueneme Channel; Hi = inner Hueneme Channel (Normark et al., 1998); K = Kalimantan; LP = La Palma (Wynn et al., 2000a); LS = Labrador Slope (Praeg and Schafer, 1989); Msm = Monterey Shepard meander; Mrl = Monterey right levee (McHugh and Ryan, 2000); MT = Manila Trough (Damuth, 1979); N = Nigeria; uR, lR = upper, lower Reserve Fan (Normark and Dickson, 1976a,b); Rp = Reynidsjup Channel (Lonsdale and Hollister, 1979); Se = Selvage (Wynn et al., 2000b); To = Toyama channel (Nakajima et al., 1998); V1–V4 = Var Fan (Migeon et al., 2000); Z1–Z3 = Zaire Fan (Migeon, 2000). Arrows indicate range of values.

terey Fan show that more sand is present on the up-current sides of successive downslope waves, so that absence of sand deposits is not a consequence of all the sand being deposited from an overspilling flow. One possibility is that the passage of the flow up the up-current side results in a reduction in flow velocity because of the local gradient, followed by re-acceleration of the flow down the down-current side. This interpretation is consistent with the observation in the Kalimantan data that sediment waves do not form where spillover from meander bends would be up the regional gradient. On the other hand, Hiscott et al. (1997) argue that the aggradation of levees on Amazon Fan is inconsistent with flow acceleration across levees, even though on the mid-fan the channel gradient is 0.3° and on the backslopes of levees the gradient is commonly 4°. Correlation of two ODP holes at Site 939, 480 m apart, on the steep flank of the Amazon Channel levee just beyond the crest (but in an area without sediment waves) shows substantial variation in sediment type (Skene, 1998), with more silts in the more proximal core, suggesting that flow expansion and deceleration is responsible for the prominent aggradational levee crest.

The observed distribution of sand and coarse silt beds in sediment waves might be accounted for by variations in tractional transport at the bed. Tractional transport would be inhibited on the up-current side of waves, where gravitational effects (e.g. pivoting to initiate grain motion or to maintain rolling) would make it more difficult to initiate grain motion. If the final stage of the sand and coarse silt deposition is tractional, and if deposition was sufficiently slow that grains moved distances of the same order as the wavelength of sediment waves, then this could account for the observed distribution of sediment. Flow velocities across the sediment waves are likely 0.5–2.0 m/s (Pirmez, 1994), implying bedload velocities of 0.2–0.3 m/s. Under these circumstances, bedload transport of one wavelength would take at most a few hours, a reasonable duration for a major turbidity current. Using the formulation in Dyer (1986, p. 119) for the threshold of motion on a slope, a 3° difference in slope would result in a 10% difference in threshold shear stress. Most

Table 2
Sediment wave attributes (see Fig. 24)

Fan	Locality	Wavelength (km)	Wave height (m)	Channel depth (m)	Channel floor width (m)	Levee width (km)	Slope regional	Reference
Amazon	930	0.57	4	45	1	4	0.01	Flood et al., 1995
	933	0.38	3	45	0.3	1	0.012	Flood et al., 1995
	3000–4000 m	1.1	< 20	80–50				this paper
Hueneme	line 12	0.15	1					this paper
	line 18	0.34	3–8					this paper
	line 1 N	0.4	3					this paper
	line 1 mid	0.55	5					this paper
	line 1 S	0.5	3					this paper
Var	group 1	5.5	46	< 50	8	10	0.035	Migeon, 2000
	group 2	1.6	20	60–200	12		0.065	Migeon, 2000
	group 3	2.2	10	60–200	12		0.02	Migeon, 2000
	group 4	0.9	7	400	8		0.02	Migeon, 2000
Zaire	general	0.75	7.5					Migeon, 2000
	zone 1	0.4	5	170				Migeon, 2000
	zone 2	1	11	180	0.5	1		Migeon, 2000
	zone 3	0.5	6	120				Migeon, 2000
	zone 4	0.4	5	60				Migeon, 2000
Monterey	Shepard meander right levee	2.5 0.3–2.1	25 10 to 20	200	1		0.014	McHugh and Ryan, 2000 Normark et al., 1980
Nigeria	offshore	0.55	10	?	1			this paper
Manila trench	up-system	3	20	200				Damuth, 1979
	down-system	0.3	5	125				Damuth, 1979
Labrador Sea	upper slope	0.5–3	10 to 30					Praeg and Schafer, 1989
	lower slope	0.5–2	5 to 20					Praeg and Schafer, 1989
Reserve	profile B–B	0.12					0.02	Normark and Dickson, 1976b
	profile E–E	0.4					0.013	Normark and Dickson, 1976b
Reynidsjup		0.5	20					Lonsdale and Hollister, 1979
Selvage		< 1.1	< 5		? > 10		0.002–0.004	Wynn et al., 2000b
La Palma		0.4–2.4	5–70	100	80		0.007–0.03	Wynn et al., 2000a
Toyama		< 3	< 70		2		0.007–0.024	Nakajima et al., 1998
Barra Fan		1.75	5				0.04	Howe, 1996

Amazon sediment waves have an absolute difference in up-current and down-current slope of about 1.5°. Even the resulting 5% difference in critical shear stress may be sufficient to concentrate granular sediment on the up-current side. In sandy bedforms, in contrast, sand distribution is influenced principally by flow separation.

Differential deposition of sand and silt beds, however, cannot account for all the observed thickness variations. The core data from Site 930 show that where the wave form aggradation is least, on the lower down-current side, sand and silt abundance is least (Hole 930B). On the other hand, the difference in total thickness of sand and silt beds between Holes 930D and 930B (< 1 m) is insufficient to account for the difference in total

thickness of sediment (< 8 m). In the upper part of the wave, formed entirely of silty mud with granular sediment beds and laminae absent, the thickness differs from 9.8 m in Hole 930B compared with 13.5 m in Hole 930D, implying significant differential deposition of cohesive silty mud flocs. It seems likely that variations in critical shear stress could also result in differential deposition of mud flocs, as bed shear stress controls adhesion and breakup of flocs.

3.3. Up-flow migration versus aggradation

On Hueneme Fan, waves showing pronounced up-flow migration occur close to the channel and are synchronous with more distal waves that show less migration and have a higher net sedimentation rate, even on down-current slopes (compare section above N′ in Fig. 10B,C). In the Niger delta example, migration of sediment waves is synchronous across the levee (Fig. 18) with distal sediment waves having a higher rate of migration than proximal waves. A similar pattern is observed for two successive sediment waves on Monterey Fan (Fig. 4), where, during the same time interval, sediment thickness on the up-current side is quite similar or increases slightly down-current. At a larger scale, sediment deposition is nearly homogeneous across the levee in the Holocene (Fig. 5B). On Var Fan, on the distal part of the ridge, sediment thicknesses on the up-current sides increase down-levee, resulting in a higher migration rate for the down-current sediment waves (Migeon et al., 2001). This is contrary to the observation that levees thin down-current. A gradual decrease in overflow velocity, accentuated by the succession of local but abrupt changes in slope gradient on each sediment wave, could explain such a down-current increase in sediment thickness.

On Amazon Fan, migration and vertical growth of waves at Site 930 was greatest during the interval when silt and sand turbidites were being deposited from the Amazon Channel at proximal levee sites such as Site 940, less when mud turbidites were deposited, and least in an interval with mud turbidites that show considerable bioturbation (Fig. 14). Migration also appears to have taken place when the waves were fed by the nearby Amazon Channel rather than when fed by the more distant Purple Channel. With the available chronology (Piper et al., 1997) there is a clear relationship between greater migration and higher sedimentation rates. Such observations also suggest that migration is enhanced by higher-velocity turbidity currents. This is consistent with Flood's (1988) observation that in contourite waves, more asymmetrical deposition patterns correspond to faster flows. On the Var Fan, phases of greater migration or greater aggradation have been correlated with supercritical and subcritical flow conditions, respectively (Migeon et al., 2000). On Amazon Fan, flow inside the Amazon Channel is likely to be slightly subcritical (Pirmez, 1994). As overbanking flows thin across the levees, flow may remain subcritical or become slightly supercritical. On Hueneme Fan, the waves with strong migration show considerable evidence for erosion on both the up-current and down-current slopes; on the down-current slope, the balance between erosional events and lower depositional rates results in net erosion in places (Fig. 10C).

3.4. Planform patterns

Three distinct planform patterns can be distinguished in the sediment-wave fields studied. In the first case, waves are essentially orthogonal to the channel trend and thus appear to have been initiated by large flows whose direction was controlled by upflow morphology, rather than spillover from an adjacent channel-levee system. On inner Hueneme levees (Fig. 7), the main levees may have acted to channelise large flows, which initiated the sediment waves above N′. In the Nigerian example, two distinct superimposed flow directions seem to be involved in sediment-wave organisation. Larger sediment waves, orthogonal to the channel trend, suggest a main flow direction parallel to the channel trend (Fig. 17) that could consist of long-distance overflow mainly controlled by the mouth of a feeder canyon. Smaller sediment waves and crest terminations adjacent to the channel, that are oriented obliquely or parallel to the channel trend (Fig. 17), sug-

gest local spreading spillover mainly controlled by the morphology of the channel and the meanders. The 3.5-kHz profiles from Sites 930 and 933 (Fig. 13) suggest that at least some of the Amazon wave fields are orthogonal to the channel.

In the second planform pattern, wave crests are parallel or slightly oblique to the channel, implying that they were initiated by flows spilling out from the channel over the levees. This organisation is observed on Pioneer, Ascension and Var fans, on levees located downstream of a sharp bend of the channel. Overflow direction is mainly constrained by the centrifugal force that acts on the channelised flow in the bend and by the local gradient slope on the levee.

In the third pattern, sediment waves mimic the meander morphology, as observed south of the Shepard meander and along the Kalimantan Channel. It suggests a construction by overflows that spread laterally around the meander. Meander morphology, i.e. their radius of curvature, is then an important factor, as suggested by the different wave field extension and organisation observed in Kalimantan Channel (Fig. 22).

Many sediment-wave fields are of substantial thickness and commonly appear to mimic underlying sediment waves. In several cases, the rate of migration of the waves decreases upwards, with the presence of more draped intervals (Figs. 2, 9 and 13B). This suggests that the regularity in wavelength and planform observed in multibeam bathymetry may be in part inherited and not necessarily an equilibrium condition that can be related to the dynamics of turbidity current flow at a particular stratigraphic level. Furthermore, caution must be exercised in interpreting waves from multibeam bathymetric or sidescan data, because it is waves that have a large height-to-wavelength ratio and a well-developed crest that will be most clearly visible on multibeam-bathymetric and sidescan-sonar data. A further problem with using sidescan sonar images is that sediment waves that have a muddy sediment drape will show insufficient backscatter variation from the low slopes of the sediment waves. Aggradational waves blanketing older sediment waves (Figs. 10A and 21) thus will be far less distinct in bathymetry or backscatter.

3.5. Relationship to initiation and character of turbidity currents

Most of the largest reported turbidite sediment waves are developed in turbidite systems in which sediment supply could have involved hyperpycnal flow from rivers, e.g. the 25 000-km^2 wave field in the South China Sea that is fed by rivers of southern Taiwan, many of which are able to generate hyperpycnal flow (Damuth, 1979; Mulder and Syvitski, 1995). The sediment waves in the South China Sea extend for more than 450 km; wavelengths are as great as 5 km and wave heights reach 50 m. There is a general decrease in both wavelength and wave height from proximal to distal position within the wave field (Damuth, 1979). Mulder and Syvitski (1995) show that hyperpycnal flow can generate turbidity currents of long duration, and entrainment can create thick, low-density flows (Piper and Savoye, 1993). Such flows are more appropriately analysed by a density gradient model (Flood, 1988) than by a two-layer turbidity current model (Normark et al., 1980). Sediment waves with mean wavelengths in excess of 1.5 km are widely developed on the high right levee of the Var Fan (Migeon et al., 2000) and sandy deposits from hyperpycnal flows are commonly described during the Holocene and at times during the Pleistocene in cores collected on prograding sediment waves (Migeon et al., 2001). The Var receives hyperpycnal flows at present (Mulder et al., 1998) and such flows would have been more abundant from cold glacial meltwater during the Pleistocene. On Bara Fan, 1.7-km-wavelength sediment waves (Howe, 1996) were presumably fed by ice-margin turbidity currents from glacial ice on the Scottish Shelf. Up to 3-km-wavelength sediment waves on the Labrador margin (Praeg and Schafer, 1989) were also deposited from turbidity currents fed from a wet ice margin.

The data from Hueneme Fan show that initiation processes of turbidity currents may have an effect on wave morphology, perhaps through changes in the size of turbidity currents, with aggradation rather than migration during intervals of hyperpycnal flow (Fig. 8A). The prominent development of sediment waves on fans fed by hy-

perpycnal flows is probably the result of such flows being unusually thick and of long duration (Piper and Savoye, 1993). In general, however, it is difficult to relate wave morphology to specific fan setting (Fig. 24). Sediment waves are formed by overbanking tops of turbidity currents, which Skene et al. (2002) have shown behave in a uniform manner independent of initiation process.

The absence of sediment waves on some turbidite fans may provide insights into their formation elsewhere. In general, sediment waves are absent on upper fan areas adjacent to deeply incised channels. For example, waves have not been seen on the upper part of Amazon Channel (Figs. 6C and 12), nor on the high eastern levee of the Eastern Valley of Laurentian Fan, nor on the proximal part of the Var Ridge, where Migeon et al. (2000) ascribed their absence to the gradient being too steep to allow sediment waves to form. Fans with highly erosional (incised) fan valleys, such as Laurentian Fan and Dume Fan offshore southern California, also lack sediment waves. Analogy with observations on Amazon Fan suggests that sediment supply may be too low or flow thickness too small in such systems to allow development of sediment waves. On the other hand, Stow and Bowen (1980) inferred flow thicknesses of hundreds of metres for deposition of proglacial clayey turbidites on the levees of Laurentian Fan. On both Laurentian Fan and the Northwest Atlantic Mid-Ocean Channel (NAMOC), where sediment waves are rare (Klaucke, 1995), the cross-levee change in sediment thickness is unusually low (Skene et al., 2002), implying thick flows. These observations suggest that turbidite systems with very thick and muddy flows result in deposits showing little thickness change with respect to distance from channels and do not produce sediment waves. One issue that remains unresolved is the effect of flow stratification and the development of internal density interfaces in the formation of turbidity-current sedument waves as proposed in the model of Flood (1988).

3.6. Recognition of sediment waves in the ancient record

The extremely low height-to-length ratio of sediment waves on levees means that they are very difficult to recognise in ancient outcrops. The concentration of sandy laminae and beds on up-current slopes that prograde up-flow provides a possible means of recognising such waves in levee sections that are continuously exposed over distances of a few kilometres. Patchy distribution of starved sand ripples and silt laminae has been described from several ancient successions (e.g. Meguma – Stow et al., 1984; Tanqua Karoo – Morris et al., 2000).

Sand beds up to 5 cm thick occur on the up-current side of sediment waves from Amazon and Monterey fans. Sand beds on waves beside the Shepard meander on Monterey Fan are at least 18 cm thick (Fig. 5C). Well-positioned cores on the more distal parts of turbidite systems with sediment waves are lacking, but on the basis of increasing thickness of sands and silts down-fan in levee sediments (Hiscott et al., 1997), sand beds up to 20 cm thick are probably common in some sediment waves.

Clemenceau et al. (2000) have described levee/overbank sand deposits at the Ram/Powell Field in the Gulf of Mexico, which extend more than 4.5 km from the channel margin. These sand units exhibit fining-upward serrated patterns on wireline geophysical logs, and in sediment cores are shown to comprise mostly laminated and thin-bedded sand layers from 0.1 to 2.5 cm, and rarely to 30 cm thick. Common sedimentary structures include climbing ripples, soft sediment deformation, sand-filled scours, wavy and lenticular rippled beds, and minor bioturbation (Clemenceau et al., 2000). These sand units produce significant hydrocarbons with peak production rates at 8.8 MBOPD and 108.1 MMCFD.

Observations on Var Fan (Piper and Savoye, 1993; Migeon et al., 2000) and on Hueneme Fan (Piper et al., 1999) show that on the lower parts of levees, sediment wave troughs may be important sites of erosion and sand deposition during spillover of sandy turbidity currents. Such sand beds on Hueneme Fan may be several metres thick (Fig. 10B) and thus may be significant reservoirs within a sediment-wave system. On Var Fan, sandy deposits on up-current flank sides

of well-developed and prograding sediment waves are up to 40 cm thick and interbedded with silty clays 5 cm thick (Migeon et al., 2001). Such sandy spillover may be less important in large passive margin systems like Amazon Fan, where the character of turbidity currents is thought to be relatively uniform (Normark and Piper, 1991; Hiscott et al., 1997). It is much more important in systems like the Var and Hueneme fans, in which the character of turbidity currents is highly variable (Mulder et al., 1998; Piper et al., 1999).

4. Conclusions

(1) Multibeam bathymetric and 3D seismic-reflection data show that fine-grained sediment-wave fields are common on the levees of submarine fans. Only fans with deeply incised fan valleys or very broad levees appear to lack sediment waves.

(2) Many sediment waves show pronounced upflow migration when they first form, but this is followed by a more aggradational phase. The wavelength of the sediment wave appears to be developed at an initiating surface and is then maintained during aggradation. Some initiating surfaces appear to be planar sand sheets, others are the irregular surface of sand bodies, whereas still others develop on muddy levees. The wavelength of many waves may thus reflect past rather than present flow conditions.

(3) Some waves develop orthogonal to channel direction and appear to have been initiated by large flows whose direction was controlled by upflow morphology, such as feeder canyons. Others develop sub-parallel to channels, particularly on meander bends and on the lower reaches of fan valleys, and result from turbidity current spillover from a channel levee system.

(4) Wave height scales with wavelength of the sediment waves. The larger waves appear to have been formed by larger turbidity currents.

(5) Sediment waves are formed by overbanking tops of turbidity currents, which behave in a relatively uniform manner independent of initiation process. However, hyperpycnal flows appear to favour the growth of large sediment waves, probably because of the thickness and duration of such flows.

(6) Waves prograde by preferential deposition on up-current sides, including deposition of thicker and more frequent sand and silt beds.

(7) Sand beds are particularly thick in sediment waves at low breaches of levees, at the outsides of meander bends, and on the lower parts of fan valleys. Sediment waves at breaches and on meander bends diminish in height rapidly away from the channel, which may be used as an exploration tool in 3D seismic interpretation. Levees without sediment waves generally lack sand and coarse silt beds.

Acknowledgements

We thank Homa Lee, David Mosher, Roger Flood, Douglas Masson and Russell Wynn for reviews that substantially sharpened our thinking. W.R.N. and D.J.W.P. thank the USGS and GSC for continuing field support over many years and the Ocean Drilling Program for the opportunity to work on Amazon Fan. Geological Survey of Canada contribution 2000301.

References

Allen, J.R.L., 1984. Sedimentary Structures: Their Character and Physical Basis. Elsevier, Amsterdam.

Brunner, C.A., Normark, W.R., 1985. Biostratigraphic implications for turbidite depositional processes on the Monterey deep-sea fan, Central California. J. Sediment. Res. 55, 495–505.

Blumsack, S.L., Weatherley, G.L., 1989. Observations of the nearby flow and a model for the growth of mudwaves. Deep-Sea Res. 40, 1327–1339.

Carter, R.M., Carter, L., 1987. The Bounty Channel system: a 55-million-year-old sediment conduit to the deep sea, Southwest Pacific Ocean. Geo-Mar. Lett. 7, 183–190.

Carter, L., Carter, R.M., Nelson, C.S., Fulthorpe, C.S., Neil, H.L., 1990. Evolution of Pliocene to Recent abyssal sediment waves on Bounty Channel levees, New Zealand. Mar. Geol. 95, 97–109.

Clemenceau, G.R., Colbert, J., Evans, D., 2000. Production results from levee-overbank turbidite sands at Ram/Powell Field, deepwater Gulf of Mexico. In: Weimer, P., Slatt, R.M., Coleman, J., Rosen, N.C., Nelson, C.H., Bouma, A.H., Styzen, M.J., Lawrence, D.T. (Eds.), Deep Reservoirs

of the World. GCSSEPM Foundation 20th Annual Bob F. Perkins Research Conference, Houston, TX, pp. 806–816.
Damuth, J.E., 1979. Migrating sediment waves created by turibidity currents in northern South China Basin. Geology 7, 520–523.
Damuth, J.E., Flood, R.D., 1985. Amazon Fan, Atlantic Ocean. In: Bouna, A.H., Normark, W.R., Barnes, N.E. (Eds.), Submarine Fans and Related Turbidite Systems. Springer, New York, pp. 415–433.
Dyer, K.R., 1986. Coastal and Estuarine Sediment Dynamics. Wiley, Chichester.
EEZSCAN 84 Scientific Staff, 1986. Atlas of the Exclusive Economic Zone, western coterminous United States, scale 1:500,000. U.S. Geological Survey Misc. Investigations Series I-1792, 152 pp.
Faugères, J.-C., Stow, D.A.V., 1993. Bottom-current controlled sedimentation: a synthesis of the contourite problem. Sediment. Geol. 82, 287–297.
Fildani, A., 1993. Evoluzione deposizionale e significato geodinamico delle torbiditi del Monterey Fan: California Centrale (USA). Laureate Thesis, Universita degli Studi di Roma 'La Sapienza', Rome.
Flood, R.D., 1988. A lee wave model for deep-sea mudwave activity. Deep-Sea Res. 35, 973–983.
Flood, R.D., Piper, D.J.W., Klaus, A., et al., 1995. Proc. ODP Init. Rep. 155, 1233 p.
Greene, H.G., Hicks, K.R., 1990. Ascension-Monterey canyon system: history and development. In: Garrison, R.E., Greene, H.G., Hicks, K.R., Weber, G.E., Wright, T.L. (Eds.), Geology and Tectonics of the Central California Coast Region, San Francisco to Monterey Bay, Pacific Section. Amer. Assoc. Petrol. Geol. Volume and Guidebook GB 67, Bakersfield, pp. 229–249.
Hein, J.R., Griggs, G.B., 1972. Distribution and scanning electron microscope (SEM) observations of authigenic pyrite from a Pacific deep-sea core. Deep-Sea Res. 19, 133–138.
Hiscott, R.N., Hall, F.R., Pirmez, C., 1997. Turbidity current overspill from the Amazon Channel: texture of the silt/sand load, paleoflow from anisotropy of magnetic susceptibility and implications for flow processes. Proc. ODP Sci. Results 155, 53–78.
Howe, J.A., 1996. Turbidite and contourite sediment waves in the northern Rockall Trough, North Atlantic Ocean. Sedimentology 43, 219–234.
Klaucke, I., 1995. The submarine drainage system of the Labrador Sea: result of glacial input from the Laurentide ice sheet. Ph.D. thesis, McGill University, Montreal, Canada.
Lee, H.J., Syvitski, J.P.M., Parker, G., Orange, D., Locat, J., Hutton, W.H., Imran, J., 2002. Distinguishing sediment waves from slope failure deposits: field examples, including the 'Humboldt slide', and modelling results. Mar. Geol. 192: S0025-3227(02)00550-9.
Lonsdale, P., Hollister, C.D., 1979. Cut-offs at an abyssal meander south of Iceland. Geology 7, 597–601.
McGann, M., 1990. Paleoenvironmental analysis of latest Quaternary levee deposits of Monterey fan, central California continental margin: Foraminifers and pollen, core S3-15G. U.S. Geological Survey Open-File Report No. 90-692.
McHugh, C.M.G., Ryan, W.B.F., 2000. Sedimentary features associated with channel overbank flow: examples from the Monterey Fan. Mar. Geol. 163, 199–215.
Migeon, S., 2000. Dunes géantes et levées sédimentaires en domain marin profond: approches morphologique, sismique et sédimentologique. Ph.D. thesis, Univ. Bordeaux I, Bordeaux.
Migeon, S., Savoye, B., Faugères, J.-C., 2000. Quaternary development of migrating sediment waves in the Var deep-sea fan: distribution, growth pattern and implication for levee evolution. Sediment. Geol. 133, 265–293.
Migeon, S., Savoye, B., Zanella, E., Mulder, T., Faugères, J.-C., Weber, O., 2001. Detailed seismic-reflection and sedimentary study of turbidite sediment waves on the Var Sedimentary Ridge (SE France): significance for sediment transport and deposition and for the mechanisms of sediment-wave construction. Mar. Pet. Geol. 18, 179–208.
Morris, W.R., Scheihing, M.H., Wickens, D.V., Bouma, A.H., 2000. Reservoir architecture of deepwater sandstones: Examples from the Skoorsteenberg Formation, Tanqua Karoo Sub-Basin, South Africa. In: Weimer, P., Slatt, R.M., Coleman, J., Rosen, N.C., Nelson, C.H., Bouma, A.H., Styzen, M.J., Lawrence, D.T. (Eds.), Deep Reservoirs of the World. GCSSEPM Foundation 20th Annual Bob F. Perkins Research Conference, Houston, TX, pp. 629–666.
Mulder, T., Syvitski, J.P.M., 1995. Turbidity currents generated at mouths of rivers during exceptional discharges to the world oceans. J. Geol. 103, 285–299.
Mulder, T., Savoye, B., Piper, D.J.W., Syvitski, J.P.M., 1998. The Var submarine sedimentary system: understanding Holocene sediment delivery processes and their importance to the geological record. In: Stoker, M.S., Evans, D., Cramp, A. (Eds.), Geological Processes on Continental Margins: Sedimentation, Mass Wasting and Stability. Geological Society Special Publication 129, pp. 145–166.
Nakajima, T., Satoh, M., Okamura, Y., 1998. Channel-levee complexes, terminal deep-sea fan and sediment wave fields associated with the Toyama Deep-Sea Channel system in the Japan Sea. Mar. Geol. 147, 25–41.
Normark, W.R., 1989. Observed parameters for turbidity-current flow in channels, Reserve Fan, Lake Superior. J. Sediment. Pet. 59, 423–431.
Normark, W.R., 1999. Late Pleistocene channel-levee development on Monterey submarine fan, central California. GeoMar. Lett. 18, 179–188.
Normark, W.R., Dickson, F.H., 1976a. Man-made turbidity currents in Lake Superior. Sedimentology 23, 815–829.
Normark, W.R., Dickson, F.H., 1976b. Sublacustrine fan morphology in Lake Superior. Am. Assoc. Pet. Geol. Bull. 60, 1021–1036.
Normark, W.R., Piper, D.J.W., 1991. Initiation processes and flow evolution of turbidity currents: implications for the depositional record. Soc. Econ. Paleotol. Mineral. Spec. Publ. 46, 207–230.
Normark, W.R., Hess, G.R., Stow, D.A.V., Bowen, A.J.,

1980. Sediment waves on the Monterey Fan levee: A preliminary physical interpretation. Mar. Geol. 37, 1–18.

Normark, W.R., Piper, D.J.W., Hiscott, R.N., 1998. Sea level effects on the depositional architecture of the Hueneme and associated submarine fan systems, Santa Monica Basin, California. Sedimentology 45, 53–70.

Piper, D.J.W., Deptuck, M., 1997. Fine-grained turbidites, Amazon Fan: facies characterisation and interpretation. ODP Sci. Results 155, 79–108.

Piper, D.J.W., Savoye, B., 1993. Processes of late Quaternary turbidity current flow and deposition on the Var deep-sea fan, north-west Mediterranean Sea. Sedimentology 40, 557–582.

Piper, D.J.W., Normark, W.R., 2001. Sandy fans - from Amazon to Hueneme and beyond. Am. Assoc. Pet. Geol. Bull. 85, 1407–1438.

Piper, D.J.W., Hiscott, R.N., Normark, W.R., 1999. Outcrop-scale acoustic facies analysis and latest Quaternary development of Hueneme and Dume submarine fans, offshore California. Sedimentology 46, 47–78.

Piper, D.J.W., Flood, R.D., Cisowski, S., Hall, F., Manley, P.L., Maslin, M., Mikkelsen, N., Showers, W., 1997. Synthesis of stratigraphic correlations of the Amazon fan. ODP Sci. Results 155, 595–609.

Pirmez, C., 1994. Growth of a submarine meandering channel-levee system on the Amazon fan. Ph.D. Thesis, Columbia University, New York.

Pirmez, C., Flood, R.D., 1995. Morphology and structure of Amazon Channel. Proc. ODP Init. Rep. 155, 23–45.

Posamentier, H.W., Kolla, V., in press. Seismic geomorphology and stratigraphy of depositional elements in deep-water settings. J. Sediment. Res.

Posamentier, H.W., Meizarwin, Wisman, P.S., Plawman, T., 2000. Deep-water depositional systems - ultra-deep Makassar Strait, Indonesia. In: Weimer, P., Slatt, R.M., Coleman, J., Rosen, N.C., Nelson, C.H., Bouma, A.H., Styzen, M.J., Lawrence, D.T. (Eds.), Deep Reservoirs of the World. GCSSEPM Foundation 20th Annual Bob F. Perkins Research Conference, Houston, TX, pp. 806–816.

Praeg, D., Schafer, C.T., 1989. Seabed features of the Labrador slope and rise near 55N revealed by SeaMARC I sidescan sonar imagery. Geological Survey of Canada Open File 2028, 28 pp.

Shepard, F.P., 1966. Meander in valley crossing a deep-sea fan. Science 154, 385–386.

Shipboard Scientific Party, 1995a. Site 930. In: Flood, R.D., Piper, D.J.W., Klaus, A., et al., Proc. ODP Init. Rep. 155, pp. 87–122.

Shipboard Scientific Party, 1995b. Site 933. In: Flood, R.D., Piper, D.J.W., Klaus, A., et al., Proc. ODP Init. Rep. 155, pp. 201–239.

Shipboard Scientific Party, 1995c. Leg synthesis. In: Flood, R.D., Piper, D.J.W., Klaus, A., et al., Proc. ODP Init. Rep. 155, pp. 17–21.

Skaloud, D.K., Cassidy, P., 1999. Exploration of the Bonga and Ngolo features in deepwater Nigeria. Am. Assoc. Pet. Geol. Bull. 83, 1340.

Skene, K.I., 1998. Architecture of submarine channel levees. Ph.D. Thesis, Dalhousie University, Halifax, NS.

Skene, K.I., Piper, D.J.W., Hill, P.S., 2002. Architecture of submarine channel levees: quantitative analysis of depositional lengthscales. Sedimentology, in press.

Stow, D.A.V., Bowen, A.J., 1980. A physical model for the transport and sorting of fine-grained sediment by turbidity currents. Sedimentology 27, 31–46.

Stow, D.A.V., Alam, M., Piper, D.J.W., 1984. Sedimentology of the Halifax Formation, Nova Scotia: Lower Paleozoic fine-grained turbidites. In: Stow, D.A.V., Piper, D.J.W. (Eds.), Fine-Grained Sediments: Deep-Water Processes and Facies. Geol. Soc. Lond. Spec. Paper 15, pp. 127–144.

Wynn, R.B., Masson, D.G., Stow, D.A.V., Weaver, P.P.E., 2000a. Turbidity current sediment waves on the submarine slopes of the western Canary Islands. Mar. Geol. 163, 185–198.

Wynn, R.B., Weaver, P.P.E., Ercilla, G., Stow, D.A.V., Masson, D.G., 2000b. Sedimentary processes in the Selvage sediment-wave field, NE Atlantic: new insights into the formation of sediment waves by turbidity currents. Sedimentology 47, 1181–1197.